MERIS 3rd data reprocessing
Validation report

Ref.: A879-NT-017-ACR

Issue: 1.0

Date: 09/10/2012

Contract N°: 21091/07/I-OL

List of Authors

	Name	Company
Prepared by the MERIS QWG members	Ludovic Bourg	ACRI-ST
	Christophe Lerebourg	ACRI-ST
	Constant Mazeran	ACRI-ST
	Véronique Bruniquel, Editor	ACRI-ST
	Kathryn Barker	ARGANS
	Jan Jackson	ARGANS
	Christopher Kent	ARGANS
	Samantha Lavender	ARGANS
	Gerald Moore	Bio-Optika
	Carsten Brockmann	Brockmann Consult
	Marc Bouvet	ESA
	Steven Delwart	ESA
	Philippe Goryl	ESA
	Jean-Paul Huot	ESA
	Ewa Kwiatkowska	EUMETSAT
	Jürgen Fisher	FUB
	Didier Ramon	Hygeos
	Roland Doerffer	HZG
	Nadine Gobron	JRC
	David Antoine	LOV
	Francis Zagolski	Parbleu
	Richard Santer	ULCO
	Jadu Dash	Univ. of Southampton
With the support of in-situ data PIs	Stan Hooker	NASA
	Vanda Brotas	Universidade de Lisboa
	Frank Muller-Karger	University of South Florida
	Susanne Kratzer	University of Stockholm
Authorised by	Philippe Goryl	ESA

Distribution List

To	Company
Philippe Goryl	ESA
MERIS QWG members	
In-situ data PIs	
+ Public distribution	

Version History

Version	Date	Changes
1.0	09/10/2012	First version

Table of Content

List of Figures

List of Tables

Acknowledgement to *in situ* data contributors

A large part of the MERIS 3rd reprocessing over the Ocean has been possible thanks to *in situ* measurements, which constitute essential independent reference data to calibrate and validate the algorithms.

The MERIS Quality Working Group is much grateful to all the scientists and associated laboratories who share their datasets within MERMAID, the validation facility used to extract MERIS matchups.

The MERMAID website http://hermes.acri.fr/mermaid contains details about the datasets, contact emails and a measurements protocols document for all available datasets (*MERIS Optical Measurement Protocols - Part A: In situ water reflectance measurements*). MERMAID validation facility is maintained by ACRI-ST, ARGANS and ESA.

In particular, the MERIS Quality Working Group thanks the following Principle Investigators and mission responsibles who currently contribute to the MERIS validation:

- Giuseppe Zibordi (Joint Research Center, Italy) for providing data at four AERONET- OC sites: the Acqua Alta Oceanographic Tower, Abu Al Bukhoosh, Gustav Dalen Tower and Helsinki Lighthouse.
    - G. Zibordi, B. Holben, I. Slutsker, D. Giles, D. D'Alimonte, F. Mélin, J.-F. Berthon, D. Vandemark, H. Feng, G. Schuster, B. Fabbri, S. Kaitala, J. Seppälä. AERONET-OC: a network for the validation of Ocean Color primary radiometric products. Journal of Atmospheric and Oceanic Technology, 26, 1634-1651, 2009.
    - G.Zibordi, J.-F.Berthon, F.Mélin, D. D'Alimonte and S.Kaitala. Validation of satellite ocean color primary products at optically complex coastal sites: northern Adriatic Sea, northern Baltic Proper and Gulf of Finland. Remote Sensing of Environment, 113, 2574-2591, 2009.
- David Antoine (Laboratoire d'Océanographie de Villefranche, France) for the BOUSSOLE dataset, used in particular for the vicarious adjustment.
    - Antoine, D. M. Chami, H. Claustre, F. D'Ortenzio, A. Morel, G. Bécu, B. Gentili, F. Louis, J. Ras, E. Roussier, A.J. Scott, D. Tailliez, S. B. Hooker, P. Guevel, J.-F. Desté, C. Dempsey and D. Adams. 2006, BOUSSOLE: a joint CNRS-INSU, ESA, CNES and NASA Ocean Color Calibration And Validation Activity. NASA Technical memorandum N° 2006 – 214147.
    - Antoine, D., P. Guevel, J.-F. Desté, G. Bécu, F. Louis, A. J. Scott and P. Bardey, 2008, The «BOUSSOLE» buoy: A new transparent-to-swell taut mooring dedicated to

marine optics: design, tests and performance at sea, *Journal of Atmospheric and Oceanic Technology*, 25, 968-989.

- David McKee (University of Strathclyde, UK) for the Bristol Channel and Irish Sea datasets.
- Kenneth Voss (NOAA) for the MOBY dataset used for the vicarious adjustment.
  - Clark, D. K., Yarborough, M. A., Feinholz, M. E., Flora, S., Broenkow, W., Kim, Y. S., Johnson, B. C., Brown, S. W., Yuen, M. & Mueller, J. L. (2003).MOBY, A Radiometric Buoy for Performance Monitoring and Vicarious Calibration of Satellite Ocean Colour Sensors: Measurements and Data Analysis Protocols. In Ocean Optics Protocols for Satellite Ocean Colour Sensor Validation, NASA Technical Memo. 2003-211621/Rev4, Vol VI, 3-34 (Eds J. L. Muller, G. Fargion and C. McClain). Greenbelt, MD.: NASA/GSFC.
- Kevin Ruddick (MUMM, Belgium) for the MUMMTriOS dataset.
  - Ruddick, K. G., V. De Cauwer, Y. Park and G. Moore (2006). Seaborne measurements of near infrared water-leaving reflectance - the similarity spectrum for turbid waters. Limnology and Oceanography 51(2): 1167-1179.
- Hui Feng (University of New Hampshire, US) and Heidi Sosik (Woods Hole Oceanographic Institution) for the AERONET-OC MVCO dataset.
  - G. Zibordi, B. Holben, I. Slutsker, D. Giles, D. D'Alimonte, F. Mélin, J.-F. Berthon, D. Vandemark, H. Feng, G. Schuster, B. Fabbri, S. Kaitala, J. Seppälä. AERONET-OC: a network for the validation of Ocean Color primary radiometric products. *Journal of Atmospheric and Oceanic Technology*, 26, 1634-1651, 2009.
- Jeremy Werdell (NASA), Ajit Subramaniam (University of Maryland, US), Dariusz Stramski (University of California, US), Greg Mitchell (University of California, US), William Balch (Bigelow Laboratory for Ocean Sciences, US), Frank Muller-Karger (University South Florida, US), Ken Carder (Professor Emeritus University South Florida, US), Norman Nelson (University of California, US), Rick Stumpf (NOAA, US), William Balch (Bigelow Laboratory for Ocean Sciences) and Stan Hooker (NASA) for the NOMAD dataset.
  - Werdell, P.J. and S.W. Bailey, 2005: An improved bio-optical dataset for ocean color algorithm development and satellite data product validation. *Remote Sensing of Environment*, 98(1), 122-140.
- David Siegel (University of California, US) for the Plumes and Blooms dataset.
- Bill Gibson (Coastal Studies Institut, LSU) and Alan Weidemann (Naval Research Laboratory, NRLSSC) for the AERONET-OC WaveCIS dataset.
- Greg Shuster (NASA GSFC) and Brent Holben (NASA GSFC) for the AERONET-OC CoveSEAPRISM dataset.
  - G. Zibordi, B. Holben, I. Slutsker, D. Giles, D. D'Alimonte, F. Mélin, J.-F. Berthon, D. Vandemark, H. Feng, G. Schuster, B. Fabbri, S. Kaitala, J. Seppälä. AERONET-OC: a network for the validation of Ocean Color primary radiometric products. *Journal of Atmospheric and Oceanic Technology*, 26, 1634-1651, 2009.

- Vanda Brotas (Universidade de Lisboa) for the Portcoast dataset.
- Vittorio Brando (CSIRO, Australia) for the AERONET-OC LJCO dataset.
- Suzanne Kratzer (University of Stockholm, Sweden) for the North-Western Baltic Sea and AERONET-OC Palgrunden dataset.

  Kratzer, S., Brockmann, C. & Moore, G. F. (2008). Using MERIS full resolution data (300 m spatial resolution) to monitor coastal waters– a case study from Himmerfjärden, a fjord-like bay in the north-western Baltic Sea. Remote Sensing of the Environment 112(5): 2284-2300.

1 Introduction

1.1 Scope of the document

This document prepared by the MERIS Quality Working Group (QWG) corresponds to the Validation Report following the 3rd MERIS data reprocessing. It aims at qualifying and quantifying the accuracy of the MERIS L2 products generated with the version 8.0 of MERIS Ground Segment prototype (MEGS), delivered to the whole community through the ODESA software (http://earth.eo.esa.int/odesa/). It is equivalent to version 6.0 of the Instrument Processing Facilities (IPF) at ESRIN.

This document completes the "3rd MERIS data reprocessing – Software and ADF updates document", ref. A879-NT-008-ACR.

1.2 Structure of the document

This document is split into the following chapters:

- This chapter introduces the document;
- Chapter 2 – Summary of the validation results;
- Chapter 3 – Validation results details.

1.3 Definitions

Statistical estimators used in this document are descrived below (x_i stands for the reference in-situ measurement, y^i stands for the MERIS measurement):

$$RPD = \frac{1}{N}\sum_{i=1}^{N}\frac{y_i - x_i}{x_i}$$

$$|RPD| = \frac{1}{N}\sum_{i=1}^{N}\frac{|y_i - x_i|}{x_i}$$

$$MAD = \frac{1}{N}\sum_{i=1}^{N} y_i - x_i$$

$$RMSE = \sqrt{\frac{1}{N}\sum_{i=1}^{N}(y_i - x_i)^2}$$

1.4 Acronyms

The definition of the acronyms used in this document is listed below:

AC	Atmospheric Correction
AD	Applicable Document
ADF	Auxiliary Data File
AMORGOS	Accurate MERIS Ortho-Geolocation Operational Software
AOT	Aerosol Optical Thickness
ARVI	Atmospherically Resistant Vegetation Index
ASH	Aerosol Scale Height
ATBD	Algorithm Theoretical Basis Document
BEAM	Basic ERS and Envisat (A)ATSR and MERIS Toolbox
BENCAL	BENGUELA current, MERIS-MODIS-SeaWiFS inter-calibration cruise
BIOSOPE	BIogeochmistry and Optics South Pacific Experiment
BOUSSOLE	BOUée pour l'acquiSition de Séries Optiques à Long Terme
BPAC	Bright Pixel Atmospheric Correction
CTP	Cloud Top Pressure
CZCS	Coastal Zone Color Scanner
DDV	Dense Dark Vegetation
DEM	Digital Elevation Model
ECMWF	European Centre for Medium-Range Weather Forecast
EO	Earth Observation
ESA	European Space Agency
ESFT	Exponential Sum Fitting Technique
FR	Full Resolution
GAME	Global Absorbing ModEl
GPS	Global Positioning System
FAPAR	Fraction of Absorbed Photosynthetically Active Radiation
FOV	Field Of View
FUB	Freie Universität Berlin
GOME	Global Ozone Monitoring Experiment
HITRAN2000	High Resolution Transmission
HZG	Helmholtz-Zentrum Geesthacht
ICOL	Improved Contrast between Ocean and Land (adjacency effect correction)
IOCCG	International Ocean Colour Coordinating Group
IOP	Inherent Optical Properties
IPF	Instrument Processing Facilities
L1, L2, L3	Level 1, Level 2, Level 3

LARS	Land Aerosol Remote Sensing
LBL	Line-By-Line
LOV	Laboratoire Océanologique de Villefranche-Sur-Mer
LUT	Look-Up Table
MBR	Maximum Band Ratio
MDS	MERIS Data Set
MDSI	MERIS Differential Snow Index
MEGS	MERIS processing chain prototype
MERIS	Medium Resolution Imaging Spectrometer
MERMAID	MERIS MAtchup In situ database
MGVI	MERIS Global Vegetation Index
MOBY	Marine Optical Buoy
MODIS	Moderate Resolution Imaging Spectrometer
MOMO	Matrix Operator MethOd
MWR	Microwave Radiometer
NIR	Near Infra-Red
NN	Neural Network
NOMAD	NASA Bio-Optical Marine Algorithm Data Set
OC4v4	4-band Ocean Colour Chlorophyll algorithm, version 4
ODESA	Optical Data processor of the European Space Agency
PCD	Product Confidence Data
PI	Principal Investigator
QWG	Quality Working Group
RMS	Root Mean Square Error
RPD	Relative Percent Difference
RR	Reduced Resolution
SAM	Standard Aerosol Model
SIO	South Indian Ocean
SOS	Successive Orders of Scattering
SPG	South Pacific Gyre
RD	Reference Document
RTC	Radiative Transfert Code
SAM	Standard Aerosol Model
SeaWiFS	Sea-Viewing Wide Field of View Sensor
SIMBADA	In situ dataset measured from the SIMBADA radiometer
SWIR	Short –Wave Infrared
SZA	Solar Zenith Angle
TOA	Top Of Atmosphere

TSM	Total Suspended Matter
ULCO	Université du Littoral et de la Côte d'Opale
VIS	Visible
VZA	View Zenith Angle
WGS	World Geodetic System
YS	Yellow Substance

2 Summary of the validation results

An exercise of validation has been carried out to quantify the accuracy of the MERIS L2 products after the 3rd reprocessing.

The Table below summarises the validation results detailed in Chapter 3 per product/flag.

The Table lists:

- All MERIS products and flags,
- The accuracy goal expected per product,
- The estimated quality following validation exercise,
- The validation method used to assess the accuracy and,
- The MERIS PIs in charge of the validation exercise.

Products are organised by processing branch (Ocean, Cloud and Land).

Flags are split into 3 categories (Surface classification, Product confidence and Science flags).

Grey lines correspond to products/flags without algorithm update/change between the 2nd and the 3rd reprocessing.

Table 1: Summary of the validation results obtained for the MERIS products and flags after the 3rd reprocessing (per branch of processing)

Processing	Product name	Goal	Estimated quality	Validation	Method / Reference	Contribution from
Ocean Products	Water Leaving Reflectance	Case 1: 0.002 RMSE in blue band (ATBD 2.7, Iss 5.1, July 2011) or 5% RPD (Gordon, 1997)	Case 1 waters, for wavelengths up to 560 nm: • RPD < 5% • RMSE < 4.10-3 Case 2 waters • RPD < 11% except at 412 nm (27.5%) • RMSE < 6.10-3	Validated	Use of the MERMAID database Comparison to SeaWiFS and MODIS for monthly time series	C. Lerebourg (ACRI-ST) C. Mazeran (ACRI-ST) E. Kwiatkowska (ESA/ESTEC)
	Algal Pigment Index I	Theoretical goal is to detect 10 classes of chlorophyll concentration with each of the 3 orders of magnitude between 0.03 and 30 mg/m3 decade, i.e. ~13%. Actual performance of OC4Me algorithm (ATBD 2.9, v4; 3 Jul 2011) is however to detect chlorophyll concentration within a factor of 0.5 to 2 (i.e. signed relative error between -50% and +100%).	RPD = -12% RMSE = 0.279 MAD = 0.086	Validated	Use of the MERMAID database Comparison to SeaWiFS and MODIS for monthly time series	C. Lerebourg (ACRI-ST) C. Mazeran (ACRI-ST) D. Antoine (LOV) E. Kwiatkowska (ESA/ESTEC)
	Algal Pigment Index II Total Suspended Matter Yellow substance	Factor 2	Site dependent, over all sites within expected range	Provisionnally validated	Comparison with CoastColour and MERMAID	R. Doerffer C. Brockmann (BC) A. Ruescas (BC)
	Photosynthetically Active Radiation (PAR)	*+/- 3%*	*+/- 3%*	*Provisionnally validated*	*Comparison to in-situ measurements and RT simulations*	*Marc Bouvet*
	Aerosol optical thickness	15% accuracy or 0.02 for moderate values (~0.1-0.2), (ATBD 2.7 Iss 4.1 Feb 2000)	Retrieved for in situ values of AOT(870) > 0.03 RMSE = 0.08 MAD = 0.04	Provisionnally validated	Use of the MERMAID database (AERONET-OC) Comparison to SeaWiFS and MODIS for monthly time series	C. Lerebourg (ACRI-ST) C. Mazeran (ACRI-ST) D. Antoine (LOV) E.Kwiatkowska (ESA/ESTEC)
	Water Vapour	*< 20% rel. To WV* *10% over glint*		*Provisionnally validated*		
	Aerosol Angström Coefficient	Not specified in ATBD	Retrieved for in situ values of AOT(870)>0.03 and alpha > 0.0 RMSE = 0.66 MAD = 0.25	Provisionnally validated	Use of the MERMAID database (AERONET-OC) Comparison to SeaWiFS and MODIS for monthly time series	C. Lerebourg (ACRI-ST) C. Mazeran (ACRI-ST) D. Antoine (LOV) E.Kwiatkowska (ESA/ESTEC)

Cloud products	*Cloud optical thickness*	*0.1 - 5.0*			
	Cloud albedo	*0.01*			
	Cloud Top Pressure	20hPa	Precision of 30hPa for low clouds, potential overestimation of cloud top-pressure for high clouds.	Validation using airborne LIDAR measurements. The validation campaign was limited to low clouds over Germany.	Dr. Rasmus Lindstrot (FUB) Dr. Rene Preusker (FUB) Prof. Jürgen Fischer (FUB)
	Cloud Type				
	Cloud reflectance				
Land products	Rayleigh corrected reflectance				NA
	Aerosol optical thickness	Standard published accuracy of aerosol products over land (i.e. MODIS) : AOT(443, 550 nm)=0.05 + 0.15* AOT	Validation against AERONET matchups: - (June 2003) MEGS 8.0: N=319 s=0.79, off=0.017, r2=0.481, rmse=0.154, Gfrac=0.53 - (June 2003) MEGS 8.0 (filtered, *(AOD) <0.1): N=243 s=1,1, off=0.039, r2=0.668, rmse=0.128, Gfrac=0.61 - (2004-2010) MODIS coll. 5: N=5448, r2=0.871, rmse=0.137, Gfrac=0.62 (Breon et al., 2011)	Validation against AERONET matchups	D. Ramon (HYGEOS) Contribution of the ESA CCI aerosol project
	Aerosol Angström Coefficient			The Ångström exponent over land is not validated and poorly correlated to AERONET	
	MGVI/FAPAR Rectified Channels	MGVI: The accuracy goal of MGVI is set to -/+ 0.05 against FAPAR estimated by radiative transfer model. When comparing to interception ground-based estimates, the goal is -/+ 0.1 Rectified Channels: As these numbers are not 'measurable' parameters, the stability over long times is set to 5%.	MGVI: The estimated quality is -/+0.1 in average when comparing with ground-based estimates. However, this value depends on the radiative transfer regime over various land cover sites. The algorithm is designed with the 'green leaf' concept and delivers instantaneous FAPAR values at time of overpass. Rectified Channels: The quality for the stability of rectified channel over	Performance assessment with FAPAR products derived from MODIS and SeaWIFS, using the same JRC algorithm. Comparisons of MGVI values against few ground-based estimates of interception (BIGfoot project and a site in Senegal). Stability of rectified channels checked over CEOS desert calibration sites and compared with MODIS surface albedo.	Nadine Gobron (EC-JRC)
	MTCI - Meris Terrestrial Chlorophyll Index - BOA vegetation index				
	Surface pressure	5 hPa	Precision of 15hPa, no bias in mid latitudes, positive bias (≤25hPa) in high latitudes, negative bias (≤25hPa) in tropics.	Comparison to surface pressure maps derived from digital elevation models, corrected for the variable sea level pressure (extracted from ECMWF)	Dr. Rasmus Lindstrot (FUB) Dr. Rene Preusker (FUB) Prof. Jürgen Fischer (FUB)
	Total Column Water Vapour (TCWV)	10% rel. To WV amount	Precision of 2 mm for cloud-free pixels for different reference data sets.	Val dation using in-situ data such as GPS and microwave radiometer measurements [Fischer et al., 2010]	Prof. Jürgen Fischer (FUB) Ronny Leinweber Hannes Diedrich

Surface classification	LAND CLOUD WATER	95%	73.5% – 99.5%	Validation using the PixBox dataset	K. Stelzer (BC) A. Ruescas (BC) C. Brockmann (BC) M. Paperin (BC)
Product confidence	PCD_1_13 - Confidence flag for water leaving/surface reflectance				
	PCD_14 - Confidence flag for water vapour				
	PCD_15 - Confidence flag for algal pigment index 1 / MGVI / CTP				
	PCD_16 - Confidence flag for YS or TSM / rectified reflectance				
	PCD_17 - Confidence flag for algal pigment index 2 / MTCI				
	PCD_18 - Confidence flag for PAR/Land surface pressure/cloud albedo				
	PCD_19 - Confidence flag for aerosol type and optical thickness / COT				
Science flags	COASTLINE - From Level 1b			Validation using the PixBox dataset	K. Stelzer (BC) C. Brockmann (BC) A. Ruescas (BC) M. Paperin (BC)
	COSMETIC - From Level 1b				
	SUSPECT - From Level 1b				
	OADB - Out Of Aerosol model DataBase:no braketing aerosol found				
	ABSOA_DUST - Desert dust absorbing aerosol/Continental absorbing aerosol				
	CASE2_S - Case 2 sediment dominated waters / Turbid water				
	CASE2_ANOM - Anomalous scattering water				
	CASE2_Y - Yellow substance loaded water				
	ICE_HAZE - ice or high aerosol load			Idem COASTLINE flag	Idem COASTLINE flag
	SNOW - snow			Idem COASTLINE flag	Idem COASTLINE flag
	MEDIUM_GLINT - Medium Glint reflectance correction applied			Idem COASTLINE flag	Idem COASTLINE flag
	BPAC_ON - Bright Pixel Atmospheric Correction				
	HIGH_GLINT - No glint correction applied			Idem COASTLINE flag	Idem COASTLINE flag
	LOW_SUN - Low sun angle				
	WHITE_SCATTERER - White scatterers within water				
	TOAVI_BRIGHT - Bright flag from TOAVI spectral tests				
	TOAVI_BAD - Bad data from TOAVI spectral tests				
	TOAVI_CSI - Cloud, snow or ice from TOAVI spectral tests				
	TOAVI_WS - Water or deep shadow from TOAVI spectral tests				

3 Validation results details

3.1 Ocean products

3.1.1 Water Reflectance

Parameters	Product type	Impacted by 3rd reprocessing	Contributor
Water Reflectance	☒ Ocean product ☐ Cloud product ☐ Land product ☐ Surface classification ☐ Product confidence ☐ Science flag	Yes : ☒ No : ☐	▪ C. Lerebourg (ACRI-ST) ▪ C. Mazeran (ACRI-ST) ▪ E. Kwiatkowska (ESA/ESTEC)

Accuracy goal	Estimated quality
Case 1: 0.002 RMSE in the blue (ATBD 2.7,v5.1, July 2011) or 5% RPD in blue band (Gordon, 1997)	Case 1 waters, for wavelengths up to 560 nm: ▪ RPD < 5.0% ▪ RMSE < 4.15×10^{-3} Case 2 waters: ▪ RPD < 12.7% ▪ RMSE < 6.2×10^{-3}

Method

The performances of MERIS Water Reflectance retrieval is based on comparison with *in situ* radiometric measurements from various sites or research projects referenced in MERMAID database (http://hermes.acri.fr/mermaid): MOBY (north Pacific), BOUSSOLE (north western Mediterranean), NOMAD (worldwide) AERONET-OC (worldwide), BristolIrishSea (western United Kingdom), MUMMTriOS (European waters), NWBalticSea (Baltic Sea) and PlumesAndBlooms (California). Size of the matchups is 5x5 RR pixels.

Case 1 and Case 2 waters were investigated separately. For both water types, relative per cent error (RPD), absolute relative per cent error (|RPD|), mean absolute difference (MAD) and root mean square error (RMSE) have been used as quality indicators.

<u>Case 1 waters</u>

Among the various *in situ* datasets available in MERMAID, MOBY, BOUSSOLE and NOMAD were selected for the validation of Case 1 waters. In addition to default flags screened before statistical computations (less than 50% pixels flagged by LAND, CLOUD, ICE_HAZE, HIGH_GLINT, MEDIUM_GLINT, PCD_19 or PCD_1_13), CASE2_ANOM and CASE2_S flags were also screened to ensure removal of optically complex pixels. Statistical screenings are maintained to default: filtered mean coefficient set to 1.5, negative reflectance removed and coefficient of variation of 0.15 at all wavelengths. Note that the graphes and statistics presented below do not include BOUSSOLE and MOBY matchups that have been used for vicarious adjustment.

Case 2 waters

AERONET-OC (AAOT, Abu Al Bukhoosh, Cove SEAPRISM, Guastav Dalen Tower, Helsinki Lighthouse, Palgrunden, WaveCIS), BristolIrishSea, MUMMTriOS, NWBalticSea and PlumesAndBlooms datasets have been selected for Case 2 water validation. AERONET -OC sites are all in coastal regions but not necessarily in turbid waters. The other selected dataset can include measurements in both coastal and oceanic regions. Only matchups in the vicinity of the coast have been selected (less than 50 km from land) but farther than 5km to avoid radiometric contamination by land. Default MERMAID flags have been selected for the results presented below (less than 50% pixels flagged by LAND, CLOUD, ICE_HAZE, HIGH_GLINT, MEDIUM_GLINT, PCD_19 or PCD_1_13). Statistical screening (filtered mean, negative reflectances and convergence criteria) are again maintained to default.

MERIS performance relatively to SeaWiFS and MODIS is also investigated on monthly time series.

Validation results

Case 1 waters

Table 2 below summarises Case 1 waters statistics. Signed relative per cent error (RPD) is within expected goal (≤ 5%) up to 560 nm. For wavebands starting at 620 nm and above, the relative errors are higher than 30%. The number of points at these bands being relatively small (<30), these values might not be reliable. Furthermore, the radiometric signal being very low at longer wavelengths in Case 1 waters, the relative error is inevitably very high. RMSE errors are slightly above expectation but results for Case 1 are in the expected order of magnitude (10^{-3}). Figure 1 presents the regression plots of MERIS versus *in situ* data where significant numbers of matchups are encountered.

Table 2: Case 1 matchup statistics

lambda	N	RPD	|RPD|	MAD	RMSE
412	234	-1.0%	13.8%	8.09E-05	4.15E-03
443	272	-5.0%	13.9%	-6.99E-04	3.13E-03
490	286	-3.8%	11.9%	-5.04E-04	2.26E-03
510	276	-3.1%	12.6%	-4.02E-04	1.66E-03
560	273	-2.1%	16.3%	-3.18E-04	1.21E-03
620	26	91.9%	134.1%	1.01E-04	8.20E-04
665	23	34.4%	106.8%	-7.99E-05	6.41E-04
681	28	72.0%	122.0%	-6.06E-05	6.14E-04
709	21	194.4%	221.8%	4.40E-05	6.67E-05
753	18	1420.2%	1435.1%	5.92E-05	9.45E-05

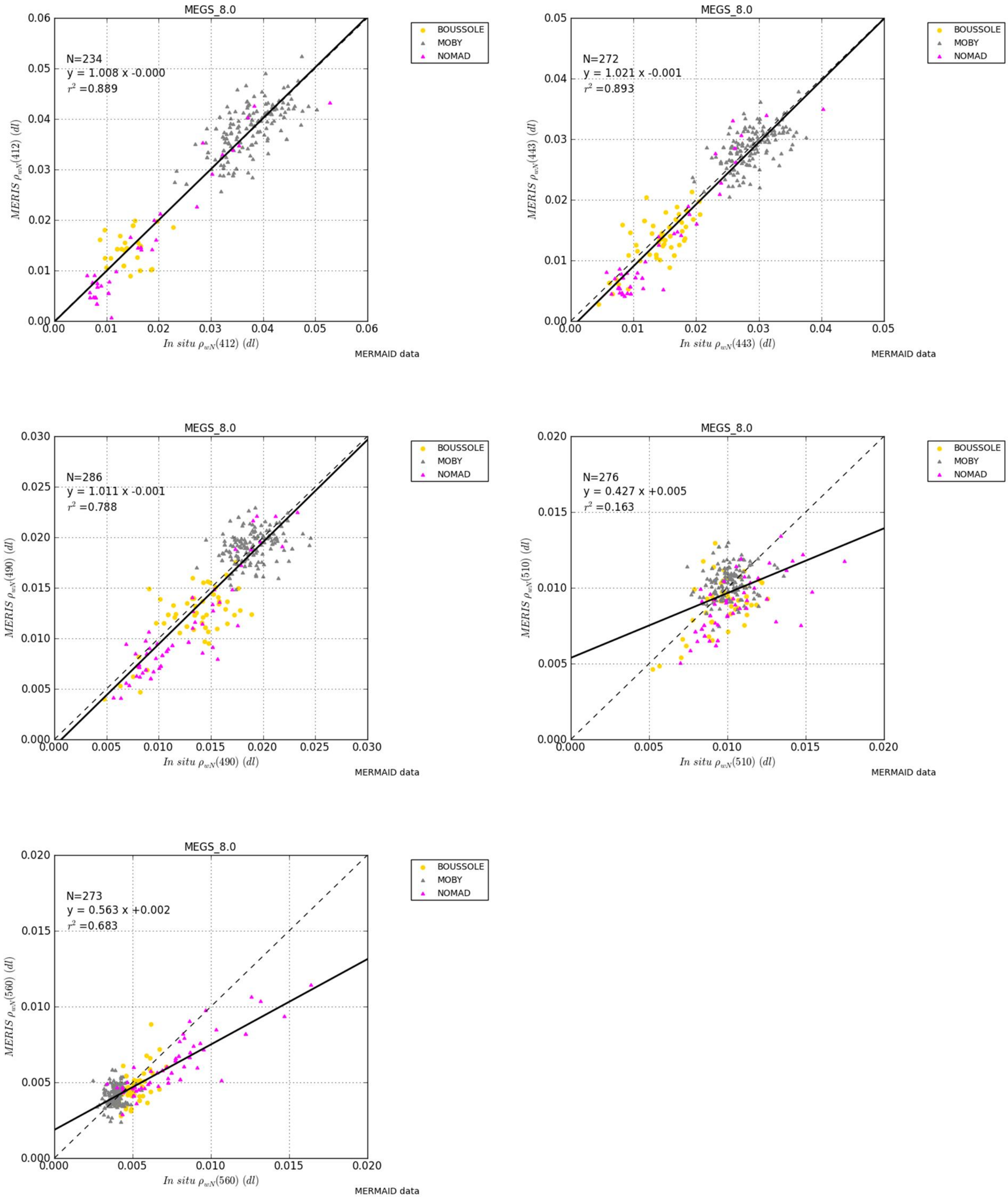

Figure 1 : Regression plots for clear waters up to 560nm

Case 2 waters

The number of points is statistically significant up to 560 nm and at 665 nm (> 80; see Table 3). At these bands, the RPD varies between -3% and -11%. An exception occurs at 412 nm with a +1.6% error, but the absolute error (MAD) is still negative, showing a general trend of overcorrection of the TOA signal in the visible As shown in Figure 2, plots are particularly scattered at 412 nm and 443 nm; RPD are therefore not meaningful at these bands.

Case 2 RMSE varies from 1.5 to 3 times the Case 1 RMSE from blue to red wavebands (Figure 3). Three bands (620, 681 and 709 nm) present significantly higher RPD than neighboring bands but few matchups are encontoured at these wavelengths. MAD values improve from blue to red wavebands with the same exceptions at 681 and 709 nm (Figure 3).

Overall, statistics improve toward red wavebands when matchup numbers are significant (Figure 2).

Table 3: Case 2 matchup statistics

lambda	N	RPD	|RPD|	MAD	RMSE
412	140	1.6%	66.4%	-2.62E-03	6.11E-03
443	202	-10.7%	34.3%	-2.52E-03	5.24E-03
490	280	-8.7%	21.3%	-1.67E-03	4.33E-03
510	83	-12.7%	21.4%	-1.70E-03	3.83E-03
560	302	-6.3%	15.9%	-1.06E-03	3.25E-03
620	16	-9.8%	19.9%	-3.15E-04	5.14E-03
665	165	-3.2%	35.8%	-4.49E-04	2.26E-03
681	26	1.1%	40.6%	3.64E-04	5.51E-03
709	9	-10.3%	29.0%	2.45E-03	1.22E-02
753	5	-42.1%	53.2%	-1.10E-03	2.51E-03
778	9	-54.3%	58.9%	-1.19E-03	1.91E-03
865	32	-47.6%	73.1%	-7.51E-04	1.19E-03

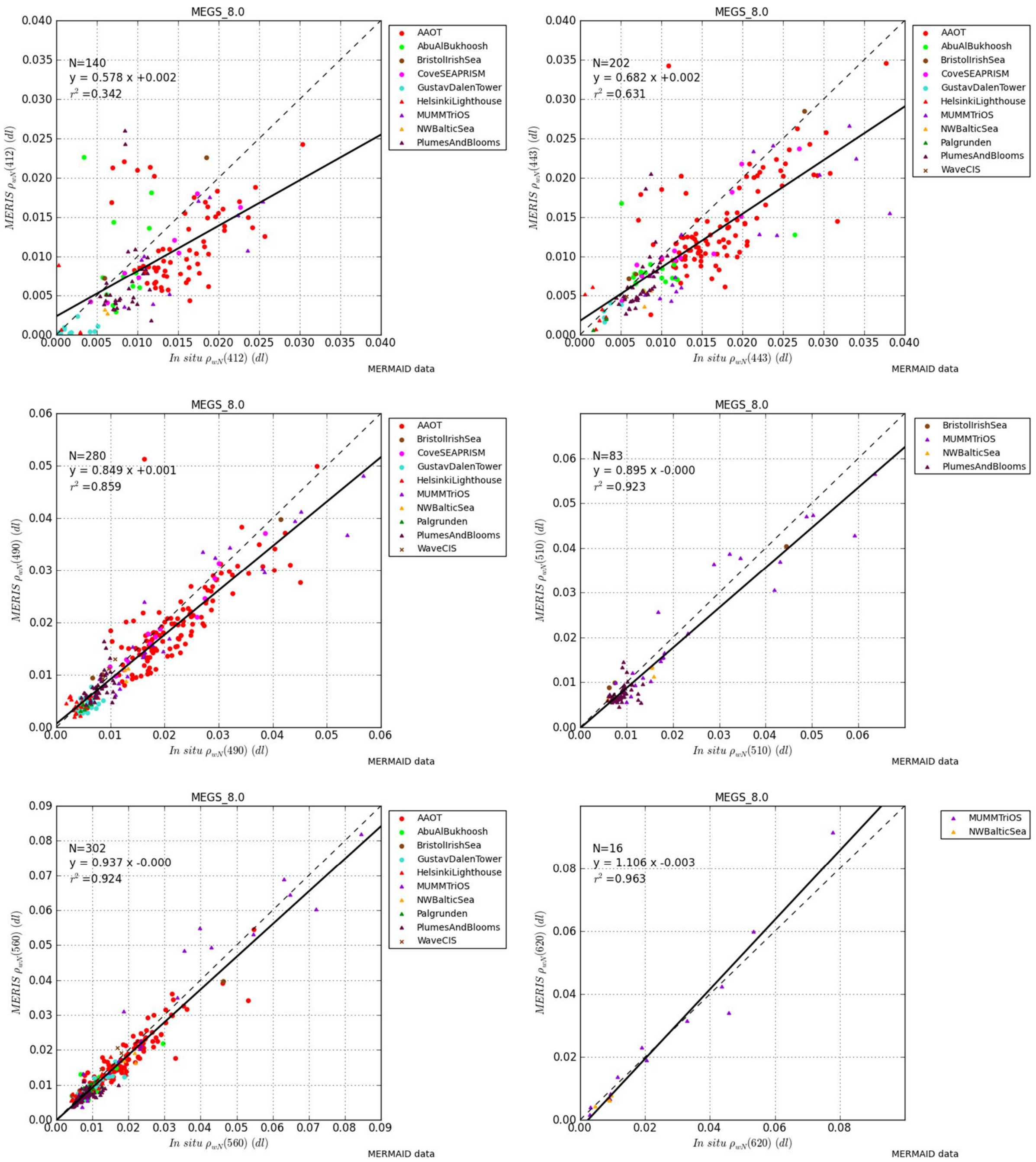

Figure 2 : Regression plots for coastal waters up to 665nm

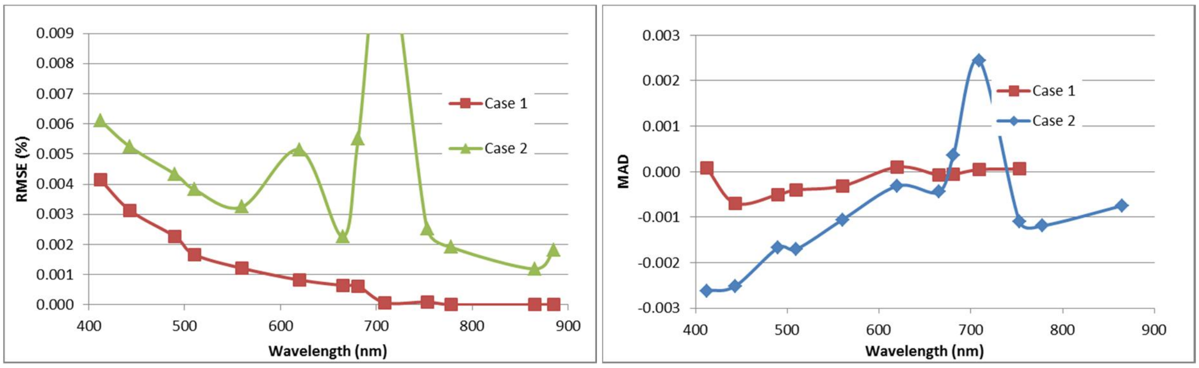

Figure 3: RMSE and MAD of case 1 and case 2 waters

In addition to validation of MERIS versus *in situ* data, an assessment of MERIS reflectance products has been performed relative SeaWiFS and MODIS-Aqua (MODIS-A) on monthly level 3 products (Figure 4 and Figure 5). Those products and statistics were processed by ACRI-ST and distributed on the GIS COOC data portal in the frame of the MULTICOLORE project, funded by CNES (MSAC/115277), using ESA ENVISAT MERIS data and NASA MODIS and SeaWiFS data; for details on calculations please refer to the Level3 intercomparison tool available at http://data.gis-cooc.org/tools-and-validation.

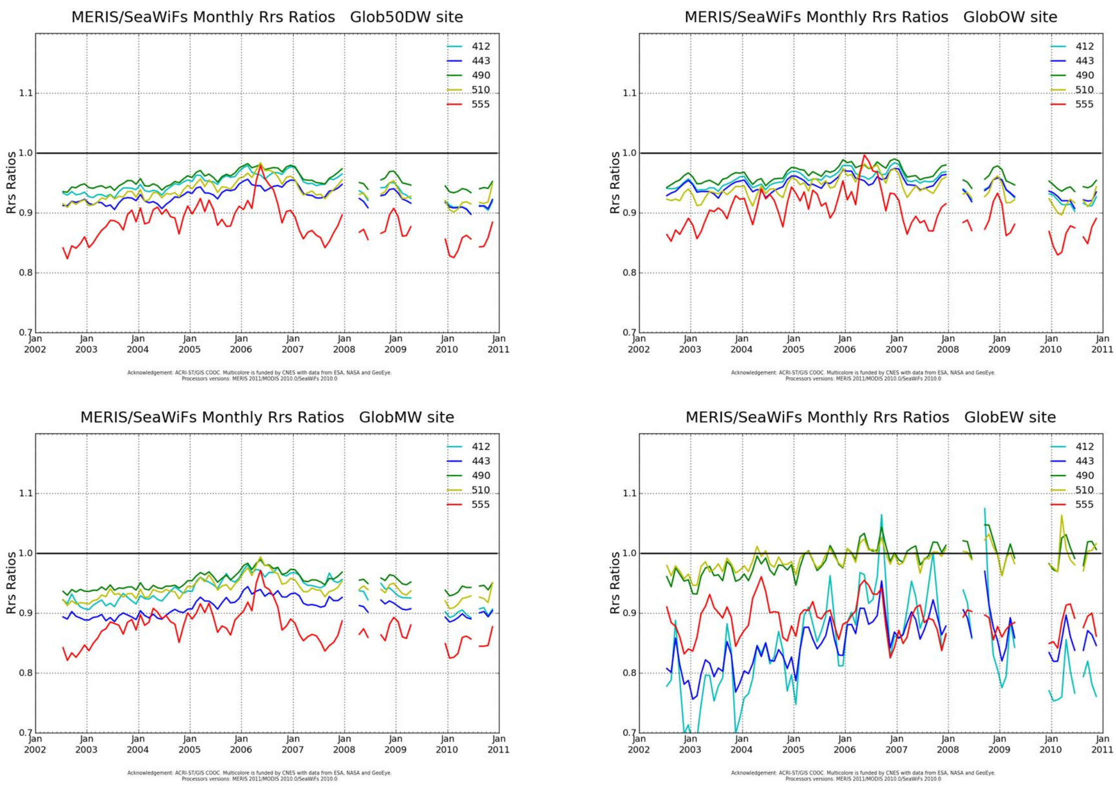

Figure 4: Monthly MERIS/SeaWiFS ratio time series for Deep water (Glob50DW ; depth < 1000 m), Oligotrophic water (GlobOW ; chl < 0.1 mg.m^{-3}), mesotrophic water (GlobMW ; 0.1 < chl < 1.0 mg.m^{-3}) and eutrophic water (GlobEW ; 1.0 < chl < 10.0 mg.m^{-3})

MERIS radiometric products are generally lower relatively to SeaWiFS products over the global world ocean. For Deep Water, oligotrophic and mesotrophic areas, the signal difference varies between 5 and 10% up to 510 nm. 555 nm signal can present higher differences (up to 18% difference – note that MERIS 560 nm band has been shifted to fit SeaWiFS waveband). The most important differences are observed on eutrophic waters i.e. coastal waters and particularly at shorter wavelength. While in the three first cases the band ratios order of magnitude remains fairly comparable, the ratios are much more variable from one band to another in case of eutrophic waters.

Similar trends can be observed relative to the MODIS signal (Figure 5) but 555 nm present a significant offset during the OCL off time period (2005-2006).

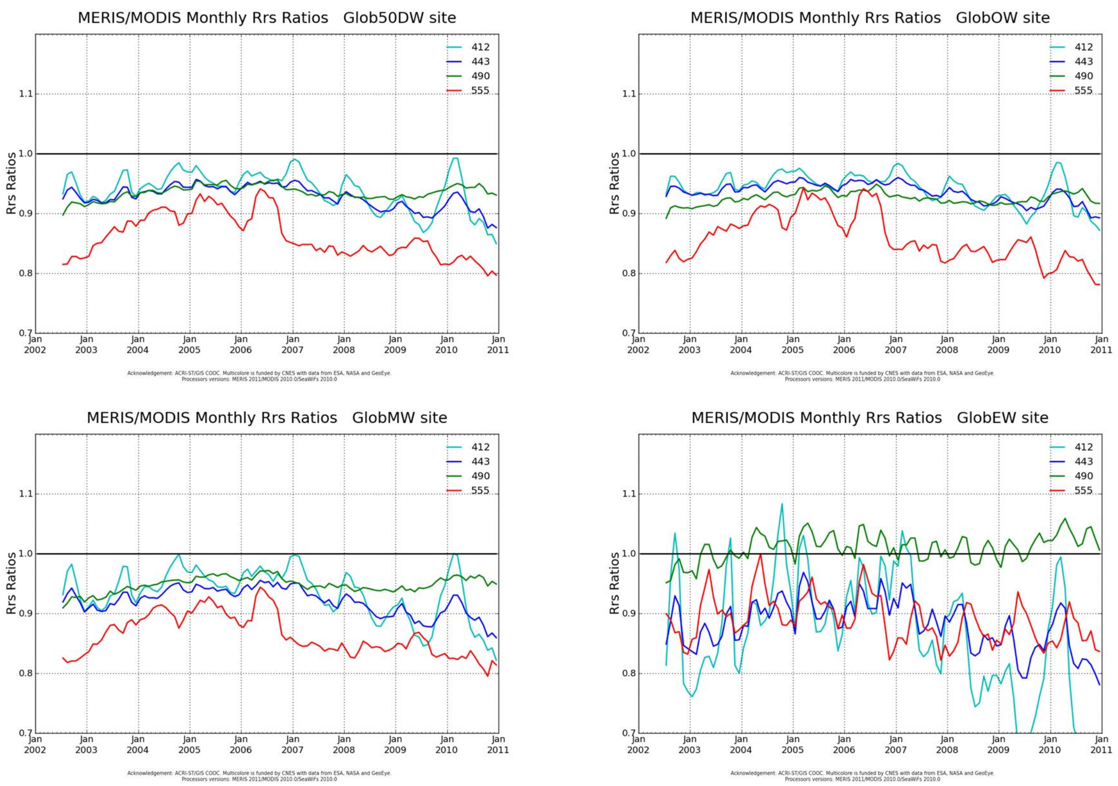

Figure 5: Monthly MERIS/MODIS ratio time series for Deep water (Glob50DW ; depth < 1000 m), Oligotrophic water (GlobOW ; chl < 0.1 mg.m^{-3}), mesotrophic water (GlobMW ; 0.1 < chl < 1.0 mg.m^{-3}) and eutrophic water (GlobEW ; 1.0 < chl < 10.0 mg.m^{-3}) ()

Reference

MERIS 3rd reprocessing, software update, 2011, ESA report, Ref A879.NT.008.ACRI-ST

Gordon H. R., 1997. Atmospheric correction of ocean color imagery in the Earth observing system era. *Journal of Geophysical Research*. 102, 17081–17106.

Acknowledgement to the MERMAID team and PIs: G. Zibordi (AAOT, Abu Al Bukhoosh, GustavDalenTower, HelsinkiLighthouse), D. Antoine (BOUSSOLE), G. Schuster & B. Holben (CoveSEAPRISM), V. Brando (LJCO), K. Voss (MOBY), H. Feng & H. Sosik (MVCO), J. Werdell & NOMAD's PIs, B. Gibson & A. Weidemann (WaveCIS),D. McKee (BristolIrishSea), Kevin Ruddick (MUMMTriOS), NWBalticSea (S. Kratzer), David Siegel (PlumesAndBlooms)

3.1.2 Algal Pigment I

Parameters	Product type	Impacted by 3rd reprocessing	Contributor
Algal 1	☒ Ocean product ☐ Cloud product ☐ Land product ☐ Surface classification ☐ Product confidence ☐ Science flag	Yes : ☒ No : ☐	▪ C. Lerebourg (ACRI-ST) ▪ C. Mazeran (ACRI-ST) ▪ D. Antoine (LOV) ▪ E. Kwiatkowska (ESA/ESTEC)

Accuracy goal	Estimated quality
Theoretical goal is to detect 10 classes of chlorophyll concentration with each of the 3 orders of magnitude between 0.03 and 30 mg/m3 decade, i.e. ~13%. Actual performance of OC4Me algorithm (ATBD 2.9, v4; 3 Jul 2011) is however to detect chlorophyll concentration within a factor of 0.5 to 2 (i.e. signed relative error between -50% and +100%).	▪ RPD (%) = - 12.0 ▪ RMSE = 0.278 ▪ MAD = 0.086

Method

The MERIS Algal_1 product is computed by the OC4Me algorithm (ATBD 2.9, v4; 3 Jul 2011) and can be validated by comparison with total chlorophyll-a measured by HPLC, noted hereafter Tchla_HPLC. The validation is thus conducted here with in situ measurements of Tchla_HPLC available in MERMAID matchup database (http://hermes.acri.fr/mermaid), also restricted to low latitudes (< 70°). This yields considering three sites: BOUSSOLE (North Western Mediterranean), NOMAD (worldwide) and PortCoast (Portuguese coasts). For these sites, the total chlorophyll-a concentration is the sum of Chlorophyll-a, Divinyl Chlorophyll-a, Chlorophyllide-a and phaeophytine-a.

For the matchups identification, 5x5 macropixels containing less than 50% of the following flags where selected: LAND, CLOUD, ICE_HAZE, HIGH_GLINT, PCD_15, CASE2_S and CASE2_ANOM. Default values are considered for other selection criteria (time difference, wind speed, solar zenith angle, scattering angle) as well as for statistical screening (convergence criteria, mean filtering and negative value removal). In addition, to remove possible coastal stations available in NOMAD dataset, matchups within 10 km of the coastline were removed. In all statistics, the chlorophyll concentration is log-tranformed.

The theoretical accuracy goal refers to identify 30 classes of chlorophyll concentration defined by $Chl[i]=0.03x10^{0.1*i}$ where i=0 to 30. This means that the ΔlogChl error, computed in log, must satisfy:

$$-0.05 \leq \Delta logChl \leq 0.05$$

or equivalently, in linear scale, a relative error of about 13%. However, the actual performance of OC4Me, when applied to *in situ* reflectance ratio, is degraded. In the plot below taken from MERIS

ATBD 2.9, we can see that for a given reflectance ratio, the chlorophyll varies within a factor of 0.5 to 2 (i.e. relative error from -50% to +100%). It means that we cannot expect better results for the MERIS product, computed on remote sensing reflectance having their own error.

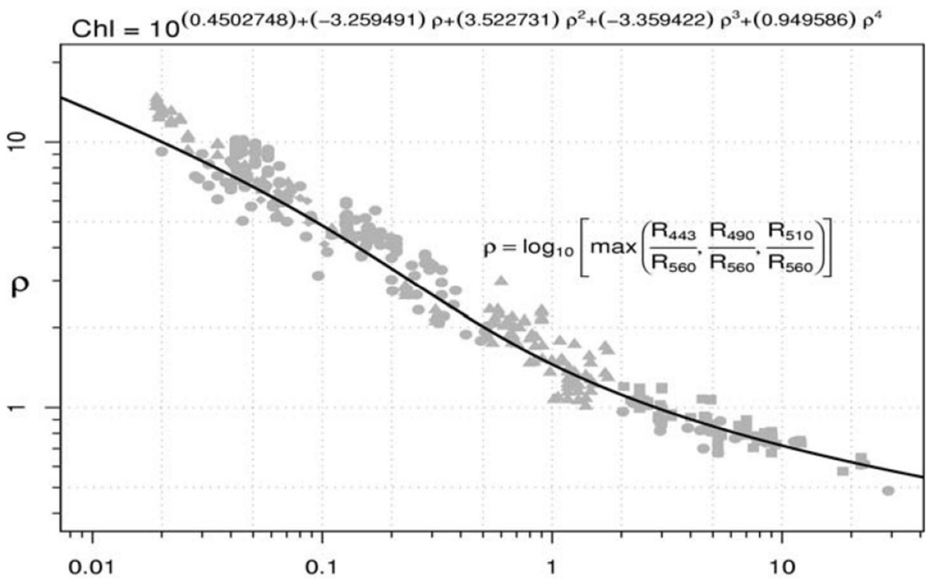

Figure 6: Performance of OC4Me against in situ measurement (reflectance and Chl) taken from MERIS ATBD 2.9, v4; 3 Jul 2011. For a given reflectance ratio, the chlorophyll can vary within a factor of 0.5 to 2.

MERIS performance relatively to SeaWiFS and MODIS is also investigated on monthly level 3 time series.

Validation results

The relative percent difference (RPD) is -12% with a 50% flag acceptance criteria. In the scatter plot below, most of the points are within the 0.5 and 2 factors discussed previously.

For comparison the same calculations have been performed accepting none of the above mentioned flags (Figure 7 and Table 4 below). While RMSE, MAD (Table 4) and regression parameters (Figure 7) remain fairly comparable, RPD is degraded with more restrictive selection criteria. This points out that RPD, being an average of signed relative errors, is not a statistical estimator as robust as RMSE or MAD.

Table 4: chlorophyll retrieval statistics

	0% flag acceptance	50% flag acceptance
N	45	62
RPD (%)	-32.0	-12.0
RMSE	0.2629	0.2781
MAD	0.1215	0.0863

The time series presented in Figure 8 demonstrates that chlorophyll evolution is very well captured by MERIS.

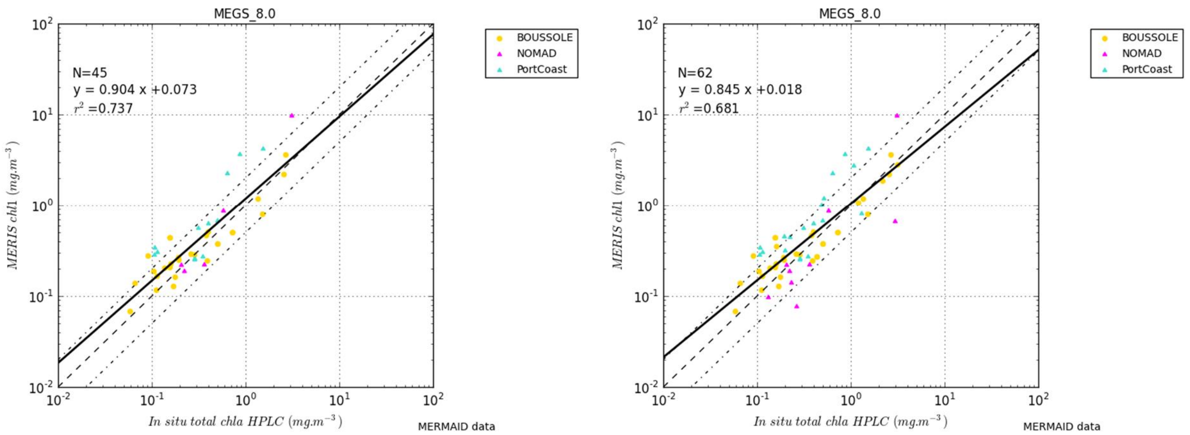

Figure 7: log/log regression of MERIS Algal 1 product versus in situ measurements; 0% flag acceptance in macropixel (left), 50% flag acceptance in macropixel (right). Dotted lines represent the accuracy goal of OC4Me (-50%; +100%).

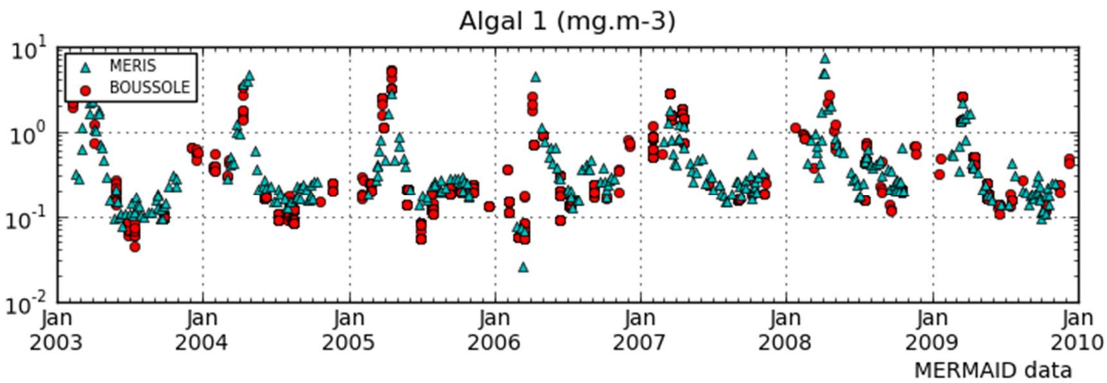

Figure 8: Time series of MERIS and BOUSSOLE

In addition to validation of MERIS product relatively to *in situ* data, an assessment of MERIS Algal_1 has been performed relatively to SeaWiFS and MODIS Chla on monthly level 3 products (Figure 9 and Figure 10). Those products and statistics were processed by ACRI-ST and distributed on the GIS COOC data portal in the frame of the MULTICOLORE project, funded by CNES (MSAC/115277), using ESA ENVISAT MERIS data and NASA MODIS and SeaWiFS data; for details on calculations please refer to the Level3 intercomparison tool available at http://data.gis-cooc.org/tools-and-validation.

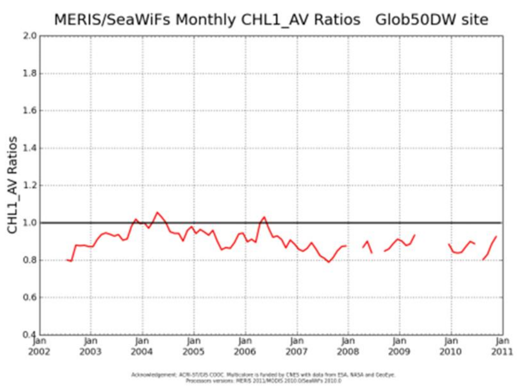

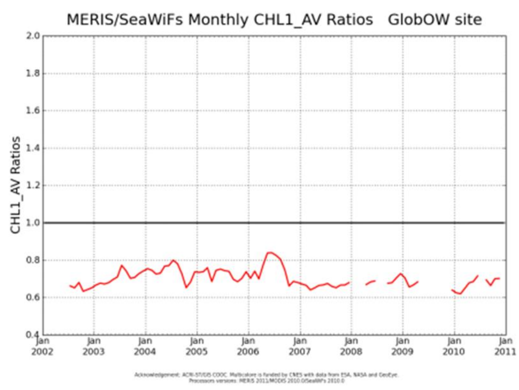

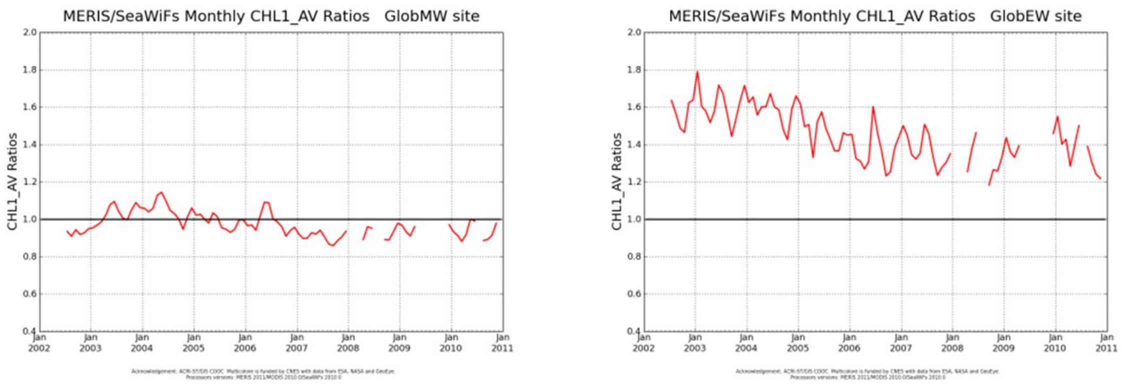

Figure 9: Monthly MERIS/SeaWiFS ratio time series for Deep water (Glob50DW ; depth < 1000 m), Oligotrophic water (GlobOW ; chl < 0.1 mg.m^{-3}), mesotrophic water (GlobMW ; 0.1 < chl < 1.0 mg.m^{-3}) and eutrophic water (GlobEW ; 1.0 < chl < 10.0 mg.m^{-3})

The general trend of MERIS Algal_1 product relative to both sensors is to underestimate low chlorophylls and overestimate high ones. This feature is totally in line with OC_4Me evolutions described in MERIS 3rd reprocessing document (Ref A879.NT.008.ACRI-ST). From oligotrophic to eutrophic water, the ratio indeed shifts from values below 1 to values above 1. On a global scale (Glob50DW), MERIS Algal_1 product difference with SeaWiFS and MODIS chlorophyll varies between +5 and -20%.

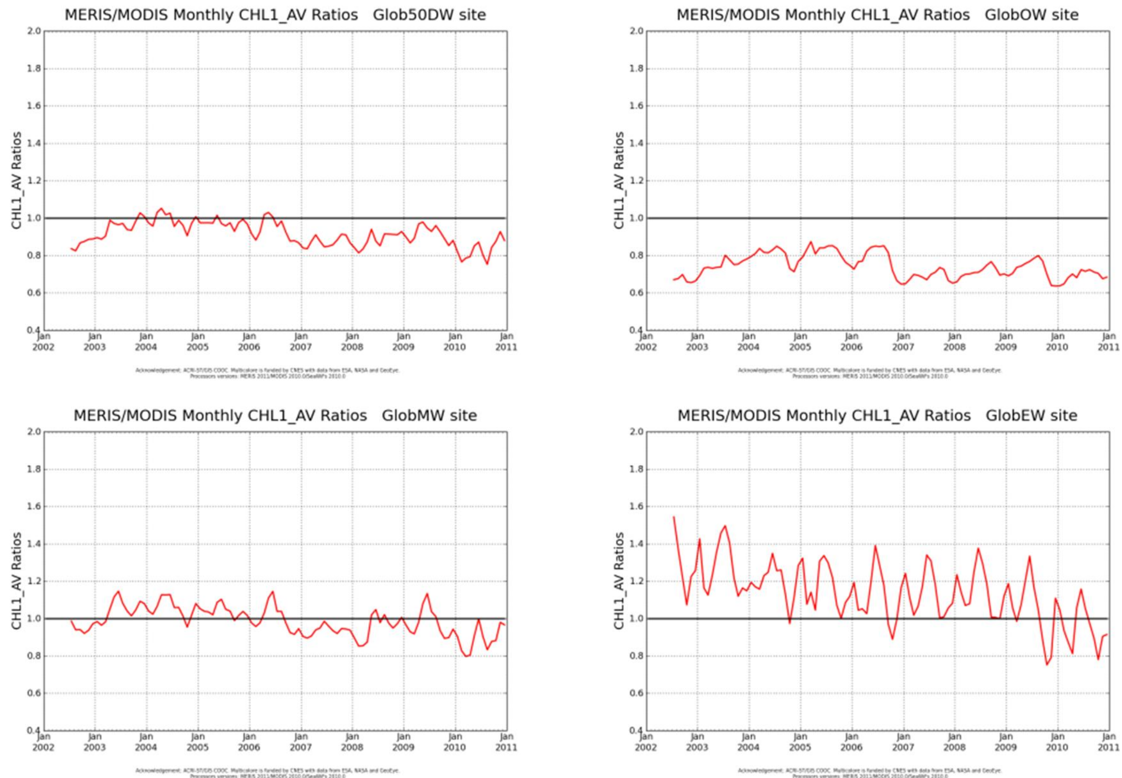

Figure 10: Monthly MERIS/MODIS ratio time series for Deep water (Glob50DW ; depth < 1000 m), Oligotrophic water (GlobOW ; chl < 0.1 mg.m^{-3}), mesotrophic water (GlobMW ; 0.1 < chl < 1.0 mg.m^{-3}) and eutrophic water (GlobEW ; 1.0 < chl < 10.0 mg.m^{-3})

Reference
MERIS 3rd reprocessing, software update, 2011, ESA report, Ref A879.NT.008.ACRI-ST

Acknowledgement to the MERMAID team and PIs: D. Antoine (BOUSSOLE), J. Werdell & NOMAD's PIs, V. Brotas (PortCoast).

3.1.3 Algal Pigment II, Total Suspended Matter, Yellow Substance

Parameters	Product type	Impacted by 3rd reprocessing	Contributor
Chlorophyll_a TSM CDOM	☒ Ocean product ☐ Cloud product ☐ Land product ☐ Surface classification ☐ Product confidence ☐ Science flag	Yes : ☒ No : ☐	▪ R. Doerffer ▪ C. Brockmann (BC) ▪ A. Ruescas (BC) ▪ K. Stelzer (BC)

Accuracy goal	Estimated quality
Factor 2	Site dependent, over all sites within expected range

Method

The Case 2 products have been compared with *in situ* data provided by CoastColour users, in the framework of the ESA DUE project CoastColour. The results are reported here to complement the analysis. Matchups have been extracted and scatter plots are used to show the correlation coefficients by parameter (Chl, TSM, CDOM). Focus is here on Case 2 waters but Algal 1 is shown for comparison as well. The CoastColour in-situ data have been collected not for the purpose of validation of satellite data, and different methods and protocols were applied. A careful quality control including consistency checks and outlier control was applied. The same method has been applied to selected sites from the MERMAID database with focus on Algal 2.

Validation results

The quantitative assessment of Case 2 products quality using MERMAID database is presented below. Before going into this, a warning should be raised that the usability of the Case 2 products is difficult because the product confidence flags (PCD_16 and PCD_17) are not properly adjusted to the new version of the algorithms. In order to overcome this problem, it is recommended to exclude the Case 2 products if one of the following conditions is true:

- Medium or high glint flag is raised
- CASE2_S flag is NOT raised
- TSM is higher than 20mg/L

By using the ODESA processor, the following criteria can be applied on the total water absorption a(λ), in order to further improve the filtering:

- 1.8*a(510)<a(412)<3.9*a(510)
- 1.5*a(490)<a(442)<1.9*a(490)

For more detailed information and discussion please refer to ODESA forum post: http://www.odesa-info.eu/forum/viewtopic.php?f=13&t=111&start=0&hilit=quinten&sid=b20804d8f9ce85efbf0ce57e1145f99c

ODESA MEGS.8 processor is used to produce the satellite measurements matching the CoastColour in-situ data. PCD flagged pixels have been excluded from the comparison. Filtering is quite conservative and the number of matchups is low in all cases: 277 for algal_2, 68 for TSM and for YS there are 115 match-ups. When possible, in cases where *in situ* data were taken with different approaches, the analyses are done separately for the different methods (i.e. fluorometric or HPLC methods for chlorophyll_a detection). The majority of the measurements providing match-ups for Algal 2 have been taken fluorometric (262) and 15 by HPLC.

Figure 11 and Figure 12 show the scatter plots, including the regression line and the correlation coefficients for the three parameters agal_2, TSM and YS. For the CoastColour sites Pearson's coefficient for algal_2 is 0.9. The algal_2 values have further a good accuracy, offset 0.2 and slope ~0.8, but with substantial dispersion and differences with regard to the measurement technique of the in-situ data. Figure 11 (right) shows the scatter plot of Algal 2, with the symbols indicating the different CoastColour sites. The correspondence between algal_2 and in-situ varies by site, but a clear tendency or grouping of the data by site is not visible.

The TSM scatter plot shows a good agreement with the in-situ data. Regression coefficient is 0.70, with slope = 0.76. The situation is less good for yellow substance. The slope is 0.65 but the dispersion is much larger than in the case of TSM, which results in a regression coefficient of 0.45.

The results of the analysis of Algal 2 using the MERMAID database are less conclusive; however, this analysis is limited by the generally low number of observations. The relationship varies substantially by site. In the NOMAD dataset the chlorophyll concentrations agrees well with the in-situ data (slope 1.02, r^2=89). At Plumes and Blooms site the correlation between Algal 2 and in-situ is much lower (r^2=0.49 and slope=0.49). At BOUSSOLE, a clear water station, both the Algal 2 product underestimates the in-situ data. The Algal 2 performs better in the clear waters at station Algarve,. However, the number of observations is too low here to draw final conclusions.

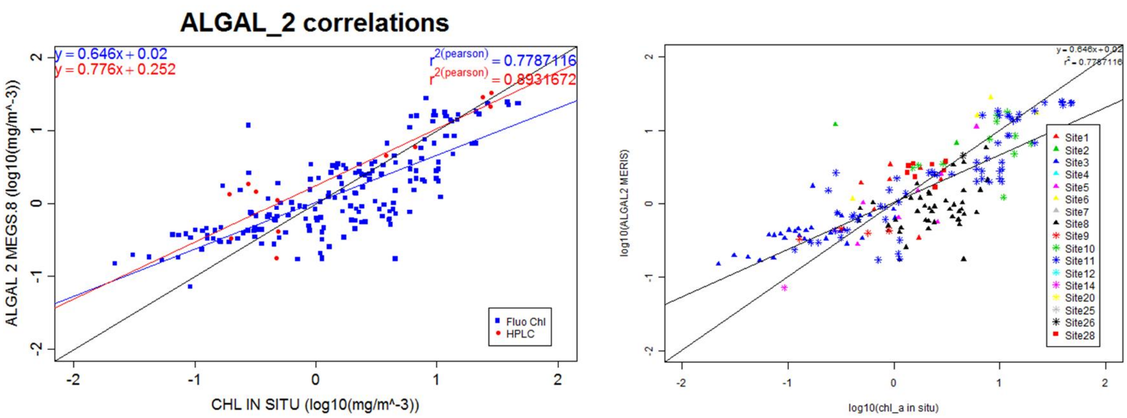

Figure 11: Algal 2 scatter plot by instrument (left) and by CoastColour site (right), all matchups, log scale

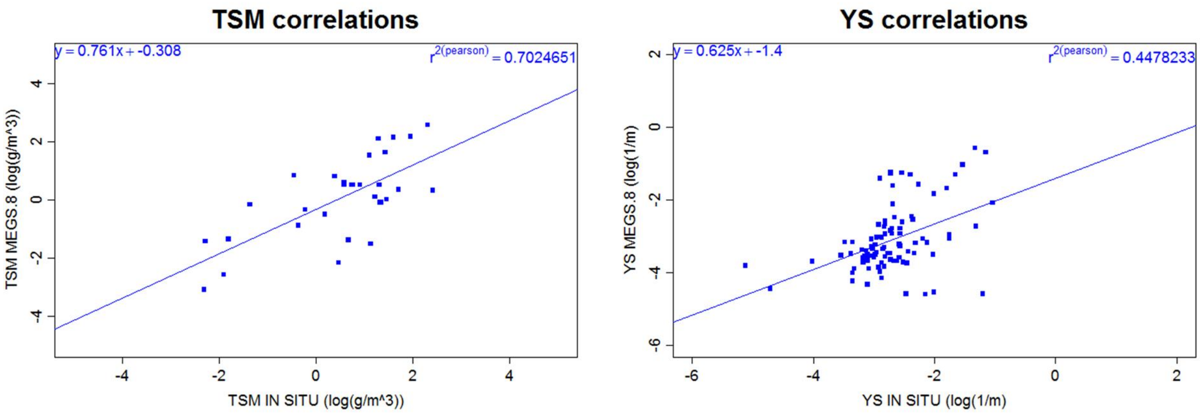

Figure 12: Scatter plots of water products, CoastColour all matchup, Algal2 vs. in situ values

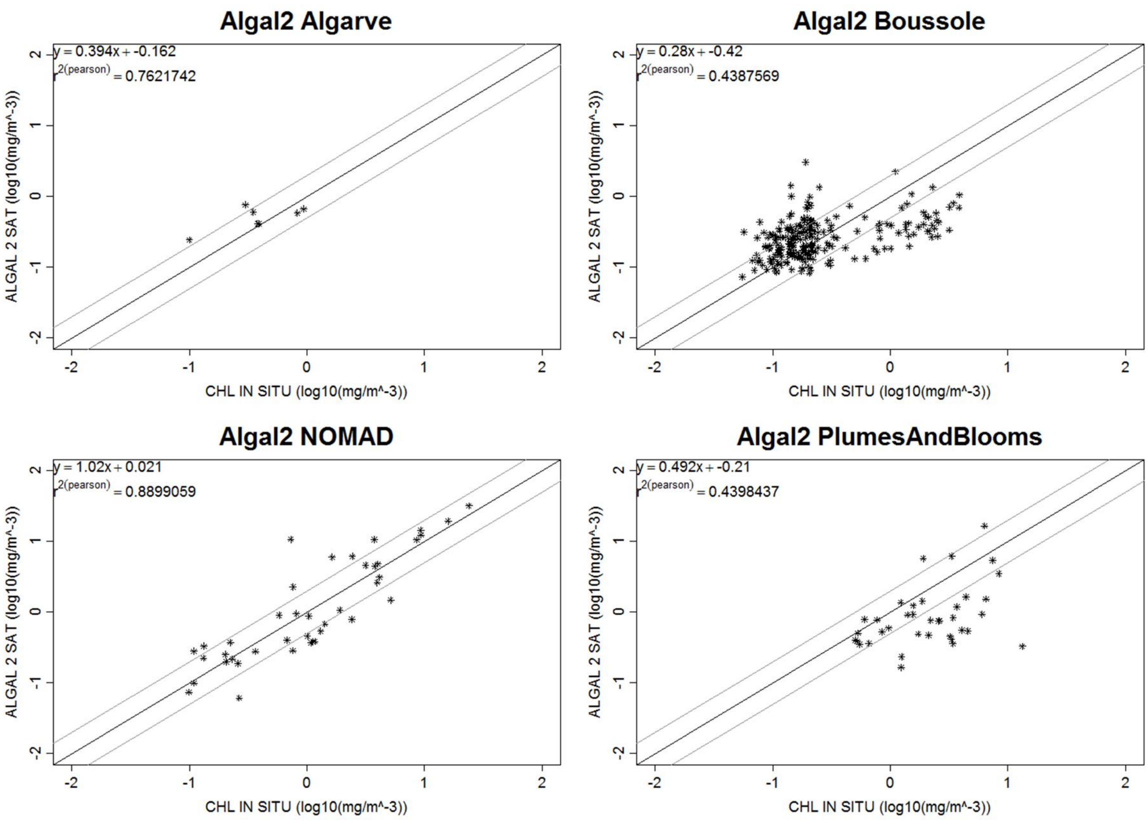

Figure 13 : Algal2 scatter plot by MERMAID site

Conclusion

First of all it has to be considered that the output of the neural network is not directly the Algal 2 product but the absorption coefficient of all pigments, from which the chlorophyll-a concentration is derived by a simple constant formula. From this conversion some of the scatter in the data has to be expected. Such a scatter is also present in data when the absorption coefficient and the chlorophyll concentration are determined from water samples. This can be seen also in the NOMAD data (Figure 12). The scatter plot of the NOMAD data base with samples from various stations around the world shows a scatter in the order of factor 2 and more. Thus, we cannot expect to be better than this in particular if we take e.g. problems of atmospheric correction over case 2 water into account.

The results of this validation indicate that the relationship between *in situ* chlorophyll concentrations and MERIS Algal 2 product is site dependent.

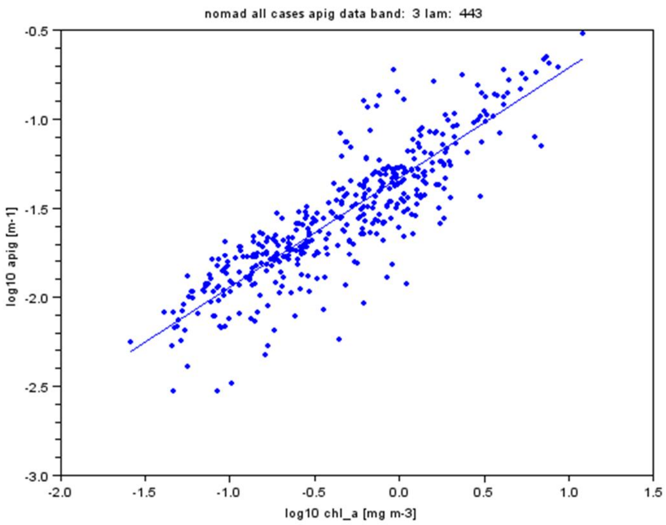

Figure 14: Relationship between log 10 of the chlorophyll concentration and log10 of the absorption coefficient at 443 nm (apig) of the NOMAD data base.

Considering all CoastColour sites the overall coefficient of determination is 0.89, which means that the algorithm provides a good retrieval of the phytoplankton absorption, apig, and the regression line shows an overall reasonable fit. The parameters of the generic conversion from apig to chlorophyll-a concentration are valid as mean coefficients. However, the individual results of the validation are quite different for different sites, including CoastColour and MERMAID sites. We thank all MERMAID data providers, ACRI-ST, ARGANS and ESA for access to the MERMAID system.

Due to the PCD_16 and PCD_17 issue, it is highly recommended to take into account the data filtering suggested in the validation result section.

Reference

DUE CoastColour in-situ database:
http://coastcolour.org/documents/TN_CC_in-situ_database_v1.4.pdf

3.1.4 Photosynthetically Active Radiation (PAR)

Parameter	Product type	Impacted by 3rd reprocessing	Contributor
Photosynthetically Available Radiation (PAR)	☒ Ocean product ☐ Cloud product ☐ Land product ☐ Surface classification ☐ Product confidence ☐ Science flag	Yes : ☒ No : ☒	Marc Bouvet (ESA)

Accuracy goal	Estimated quality
The claimed accuracy for the PAR produt is +/- 3% according to the MERIS ATBD 2.18 from Aiken et al. (see R-1)	

Method

The MERIS PAR product is described in the MERIS ATBD 2.18 from Aiken and Moore (see R-1). The MERIS PAR product is generated via a Look-Up-Table (LUT). The entries of this LUT are: the solar zenith angle, the aerosol optical thickness at 865 nm (AOT_865), the Angstrom exponent between 778 nm and 865 nm (alpha_865_778), the ozone concentration (O3) and the column water vapour (WV). These inputs are taken from the navigation data (solar zenith angle), the L2 processing (AOT_865, alpha_865_778 and WV) or from auxiliary data (O3).

The accuracy claimed by the ATBD authors for the PAR derived from the LUT is +/- 3%. This figure is however not backed up in the ATBD by validation results.

The PAR LUT generation is based on the spectral solar irradiance model for cloudless maritime atmospheres from Gregg and Carder (see R-3). These authors validated their model against in-situ measurements of spectral solar irradiance. We report their results in the next section.

In addition, Bouvet *et al.* (see R-2) compared the MERIS PAR product from the 2nd reprocessing to:

- A PAR computed with the 6S radiative transfer code with similar input to those of the MERIS PAR LUT.
- A PAR derived from shortwave radiation measurements at the Tropical Atmosphere Ocean array of moored buoys

These results are hereafter summarized.

It should be noted that there is no change between the 2nd and 3rd reprocessing as far as the PAR LUT is concerned. However, for a given MERIS acquisition, the inputs to the PAR LUT derived from the 2nd and 3rd reprocessing differ due to various reasons: update of the L1b calibration, L2 algorithmic changes and the consolidation of auxiliary data. Consequently, hereafter are also reported the results of the direct inter-comparison of PAR products from the 2nd and 3rd reprocessing.

Validation results

Gregg and Carder (see R-3) claim their model agreed "*spectrally with observed surface spectral irradiances to within +/- 6 % and as integrated PAR to within +/- 5.1 %*". Aiken and Moore claim an accuracy of +/- 3% on the PAR in the MERIS ATBD 2.18. This figure might be an educated guess since there is no validation of the MERIS PAR product in the MERIS PAR ATBD.

Bouvet *et al.* (see R-2) reported the results of the comparison of the MERIS PAR product from the 2nd reprocessing to:

- A PAR computed with the 6S radiative transfer code with similar input to those of the MERIS PAR LUT: the MERIS PAR showed a +1.9 % bias with a standard deviation of less than 0.8% on 28 samples
- A PAR derived from shortwave radiation measurements at the Tropical Atmosphere Ocean array of moored buoys: the MERIS PAR showed a -0.9% bias with a standard deviation of 5.7 % on only 8 matchups

To assess the impact of the changes on the inputs to the PAR LUT on the PAR product itself, data from the 3rd and 2nd reprocessing were compared. An example is provided in the figures hereafter. On this example, the product coverage is slightly modified not only by the changes is valid input data (mainly AOT_865, alpha_865_778, WV) but also by the modification to the pixel identification scheme in the 3rd reprocessing, and in particular the cloud detection. The relative changes are generally small, of about few percents which is within the uncertainty of the product.

Conclusion:

Changes to the MERIS PAR product are minor between the 2nd and 3rd reprocessing and are comparable to the expected and measured uncertainty of the product.

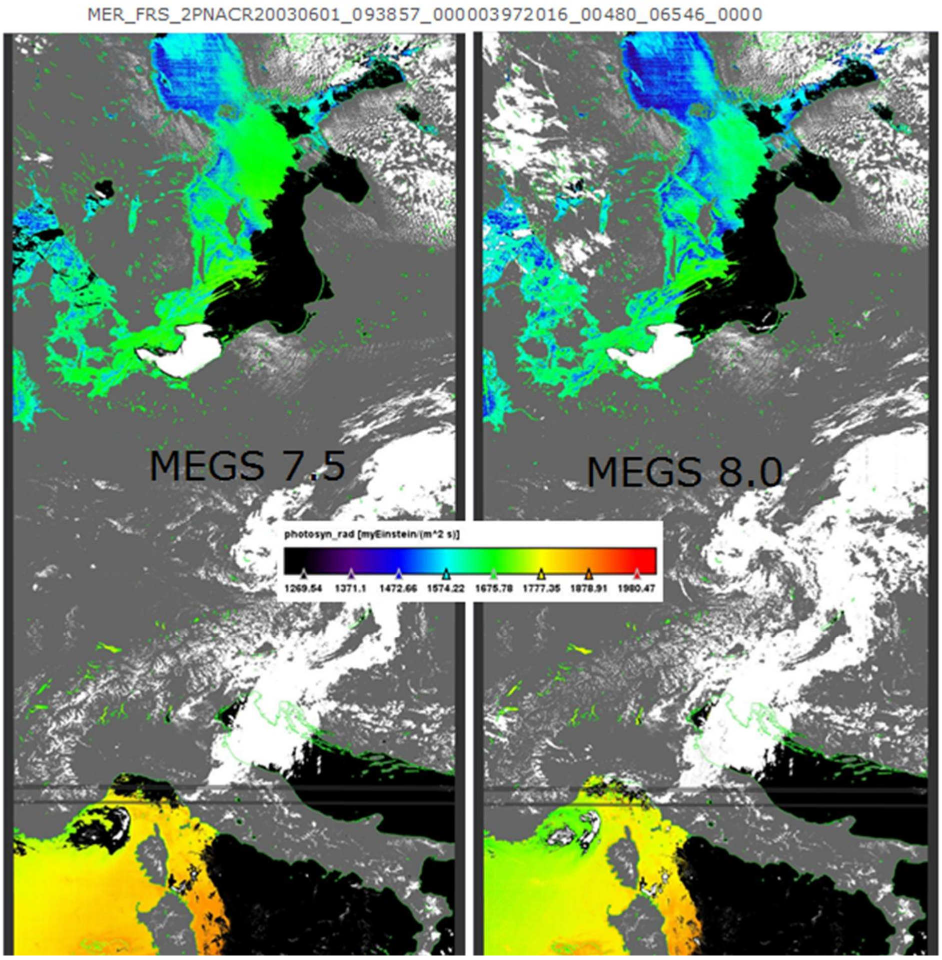

Figure 15: PAR product from the 2nd (left) and 3rd (right) reprocessing derived for the same MERIS acquisition.

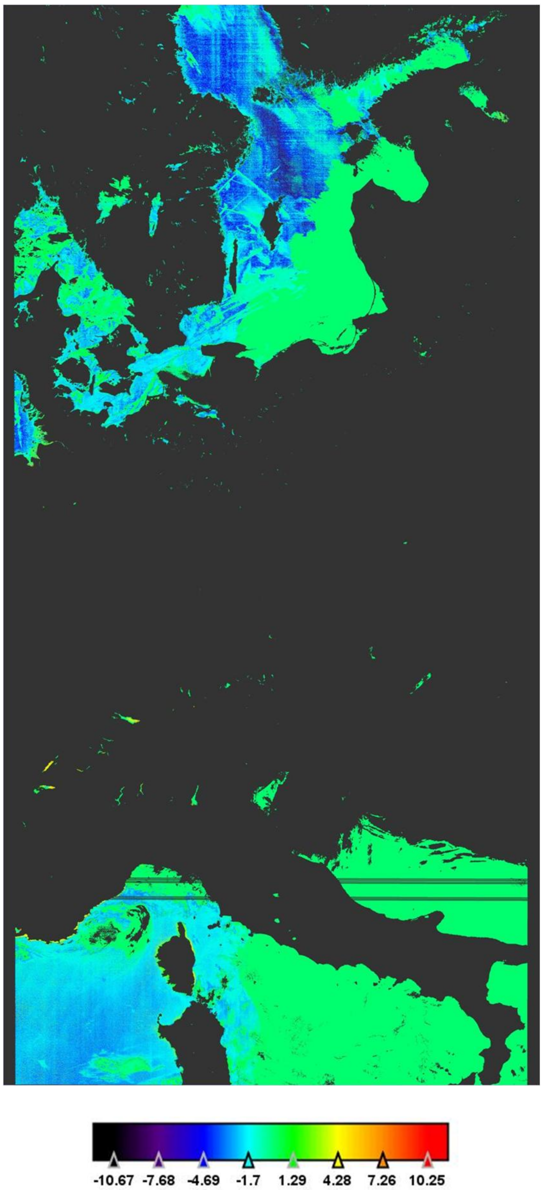

Figure 16: Relative difference in % between the PAR product from the 2nd and 3rd reprocessing

References

R-1: Aiken J., Moore G., MERIS ATBD 2.18 - Photosynthetically Available Radiation (PAR)

R-2: Bouvet M.. The MERIS Photosynthetic Available Radiation – A product assessment, MAVT 2006, (http://envisat.esa.int/workshops/mavt_2006/MAVT-2006-1005_MBouvet.pdf)

R-3: Gregg, W. W. & Carder, K. L. (1990): A simple spectral solar irradiance model for cloudless marine atmospheres.

3.1.5 Aerosol Optical Thickness

Parameters	Product type	Impacted by 3rd reprocessing	Contributor
Aerosol Optical Thickness at 865 nm (AOT865)	☒ Ocean product ☐ Cloud product ☐ Land product ☐ Surface classification ☐ Product confidence ☐ Science flag	Yes : ☒ No : ☐	▪ C. Lerebourg (ACRI-ST) ▪ C. Mazeran (ACRI-ST) ▪ D. Antoine (LOV) ▪ F. Zagolski (PARBLEU) ▪ E. Kwiatkowska (ESA/ESTEC)

Accuracy goal	Estimated quality
15% accuracy or 0.02 for moderate values (~0.1-0.2), (ATBD 2.7 Iss 4.1 Feb 2000)	Retrieved for *in situ* values of AOT(870) > 0.03 ▪ RMSE = 0.08 ▪ MAD = 0.04

Method

AERONET-OC data available in MERMAID were used to derive the AOT quality. Owing to the vicinity of the coast and the consequent optical complexity of AERONET-OC sites, the matchup selection has been very rigorous for the purpose of parameter quality computation. Through the MERMAID interface, 5x5 macropixels containing none of the following flags where selected: LAND, CLOUD, ICE_HAZE, HIGH_GLINT, PCD_19, OADB.

With these results, we compare the aerosol optical thickness measured by MERIS at 865nm to *in situ* measurements of aerosol optical thickness measured on AERONET-OC sites at 870nm. In addition to flag selection, *in situ* and satellite measurements of AOT have been filtered to remove the values lower than 0.03. The same filtering procedure is applied the Angström exponent.

MERIS retrieval relative SeaWiFS and MODIS is also investigated on monthly level 3 time series.

Validation results

MERIS product is generally overestimated with respect to *in situ* AOT(870) measurements (Figure 17). The absolute error histogram (Figure 17, right) presents more precisely the positive bias on AOT.

On the validation of AOT(865), we must point out that the *in situ* dataset used for the assessment is limited to AERONET-OC and therefore coastal sites with complex atmospheric optical properties. The statistics presented above might not be representative of the behaviour of MERIS atmospheric corrections on a global scale. Furthermore, it is worth mentioning that AOT is a by product of atmospheric corrections and not a product in itself. It is therefore an indicator of atmospheric correction quality. This validation exercice of AOT confirms the results of section 3.1.1: water leaving reflectances in the coastal region tend to be under estimated.

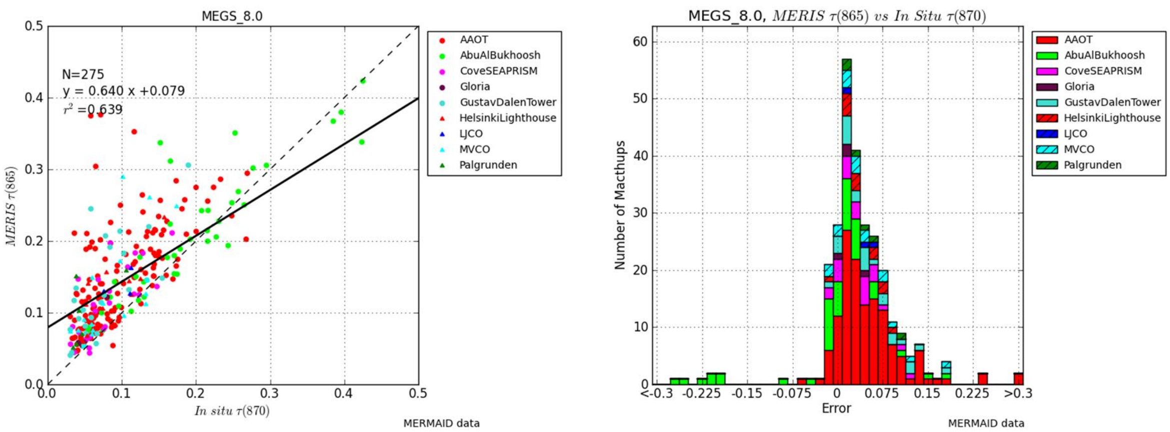

Figure 17: Aerosol Optical Thickness retrieval statistics; filtering on small AOT values (AOT(865) > 0.03); scatter plot (left), Absolute Difference (right).

Figure 18 and Figure 19 present the AOT(865) ratio of MERIS to SeaWifs and MERIS to MODIS. These ratios are calculated on monthly level3 product. Those products and statistics were processed by ACRI-ST and distributed on the GIS COOC data portal in the frame of the MULTICOLORE project, funded by CNES (MSAC/115277), using ESA ENVISAT MERIS data and NASA MODIS and SeaWiFS data; for details on calculations please refer to the Level3 intercomparison tool available at http://data.gis-cooc.org/tools-and-validation. The ratios of MERIS to MODIS present a clear seasonal signal except for eutrophic, i.e. coastal waters. The MERIS to MODIS signal remains very stable throughout the studied time period. The seasonal signal is not so clear for MERIS to SeaWiFS ratios except for oligotrophic waters and the amplitude of the signal tends to increase with time for eutrophic waters.

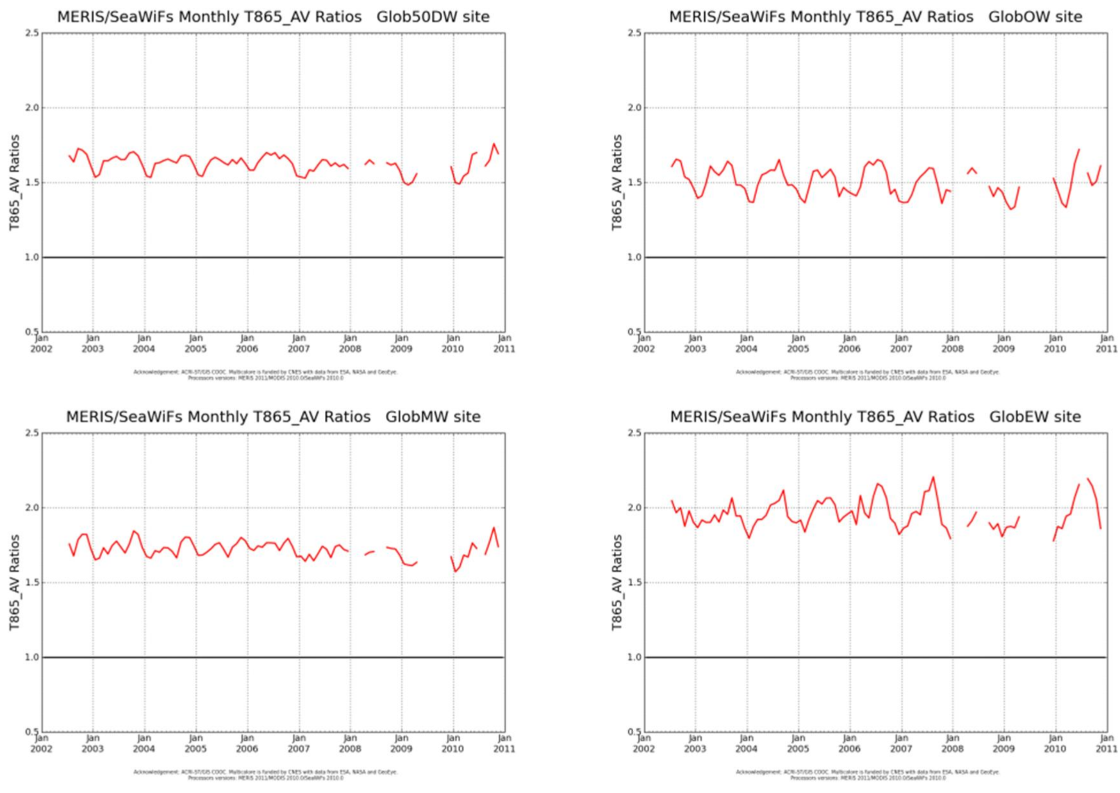

Figure 18: Monthly MERIS/SeaWiFS ratio time series for Deep water (Glob50DW ; depth < 1000 m), Oligotrophic water (GlobOW ; chl < 0.1 mg.m^{-3}), mesotrophic water (GlobMW ; 0.1 < chl < 1.0 mg.m^{-3}) and eutrophic water (GlobEW ; 1.0 < chl < 10.0 mg.m^{-3})

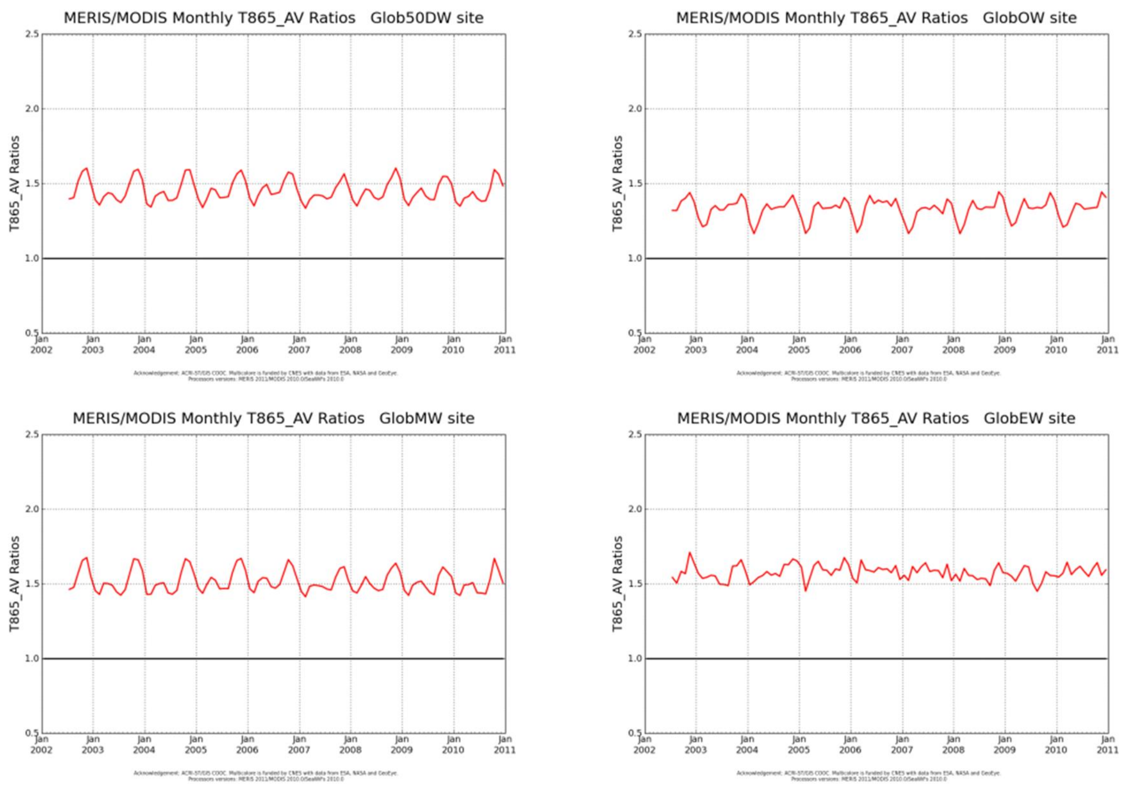

Figure 19: Monthly MERIS/MODIS ratio time series for Deep water (Glob50DW ; depth < 1000 m), Oligotrophic water (GlobOW ; chl < 0.1 mg.m^{-3}), mesotrophic water (GlobMW ; 0.1 < chl < 1.0 mg.m^{-3}) and eutrophic water (GlobEW ; 1.0 < chl < 10.0 mg.m^{-3})

References

MERIS 3rd reprocessing, software update, 2011, ESA report, Ref A879.NT.008.ACRI-ST

Acknowledgement to the MERMAID team and PIs: G. Zibordi (AAOT, Abu Al Bukhoosh, Gloria, GustavDalenTower, HelsinkiLighthouse), G. Schuster & B. Holben (CoveSEAPRISM), V. Brando (LJCO), H. Feng & H. Sosik (MVCO), S. Kratzer (Palgrunden).

3.1.6 Aerosol Angström Coefficient

Parameters	Product type	Impacted by 3rd reprocessing	Contributor
Alpha	☒ Ocean product ☐ Cloud product ☐ Land product ☐ Surface classification ☐ Product confidence ☐ Science flag	Yes : ☒ No : ☐	▪ C. Lerebourg (ACRI-ST) ▪ C. Mazeran (ACRI-ST) ▪ E. Kwiatkowska (ESA/ESTEC)

Accuracy goal	Estimated quality
Not specified in ATBD	Retrieved for *in situ* values of AOT(870)>0.03 ▪ RMSE = 0.66 ▪ MAD = 0.25

Method

AERONET-OC data available in MERMAID were used to derive the Angström coefficient quality. Owing to the vicinity of the coast and the consequent optical complexity of AERONET sites, the matchup selection has been very rigorous for the purpose of parameter quality computation. Through the MERMAID interface, 5x5 macropixels containing none of the following flags where selected: LAND, CLOUD, ICE_HAZE, HIGH_GLINT, PCD_19, OADB.

In this section, we compare the results of Angström coefficient measured by MERIS (Alpha) to in-situ Angström coefficient derived from the aerosol signal using either 870 and 675 or 870 and 665 nm measurements. In addition to flag selection, *in situ* and satellite AOT measurements have been filtered to remove the values lower than 0.03. The same filtering procedure is applied to the AOT(865) validation.

MERIS performance relative SeaWiFS and MODIS is also investigated on monthly level 3 time series.

Validation results

The spectral slope of the aerosol is generally overestimated as presented in Figure 20. As for AOT(865), we must point out that the in-situ dataset used for the Alpha product quality assessment is limited to AERONET-OC sites. These sites are in the coastal zone and therefore present complex atmospheric optical properties. The statistics presented above might not be representative of the behaviour of MERIS atmospheric corrections on a global scale.

Figure 21 and Figure 22 present the Angström coefficient ratio of MERIS to SeaWifs and MERIS to MODIS time series. These ratios are calculated on monthly level3 product. Those products and statistics were processed by ACRI-ST and distributed on the GIS COOC data portal in the frame of the MULTICOLORE project, funded by CNES (MSAC/115277), using ESA ENVISAT MERIS data and NASA MODIS and SeaWiFS data; for details on calculations please refer to the Level3 intercomparison tool available at http://data.gis-cooc.org/tools-and-validation. MERIS to SeaWiFS ratios present a decreasing trend throughout the time series. A seasonal signal can be identified on both MERIS to MODIS and MERIS to SeaWiFS ratios. MERIS to MODIS ratios are more stable throughout the times series although a slight offset can be identified, especially on oligotrophic waters, during the OCL off time period (2005-2006).

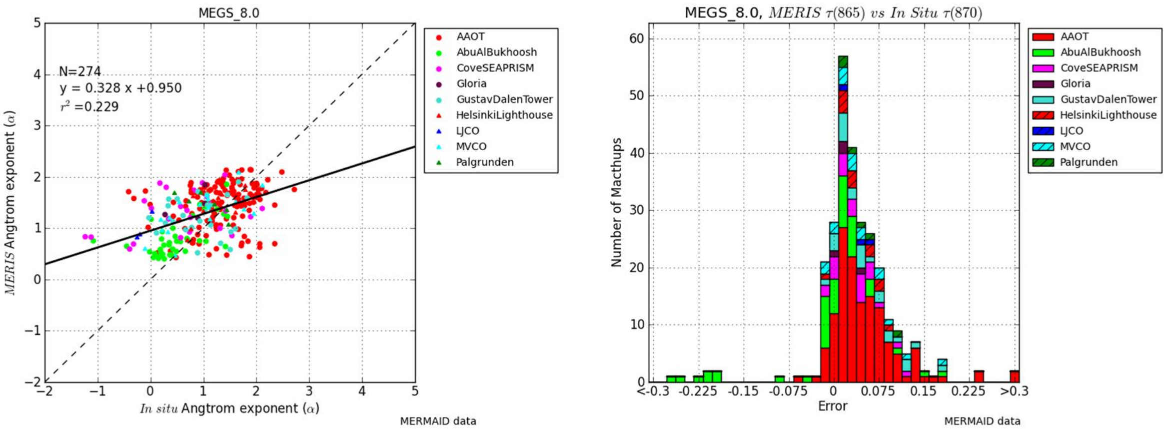

Figure 20: Alpha retrieval statistics; filtering on small AOT values (AOT(865) > 0.03) ; scatter plot (left), Absolute Difference (right).

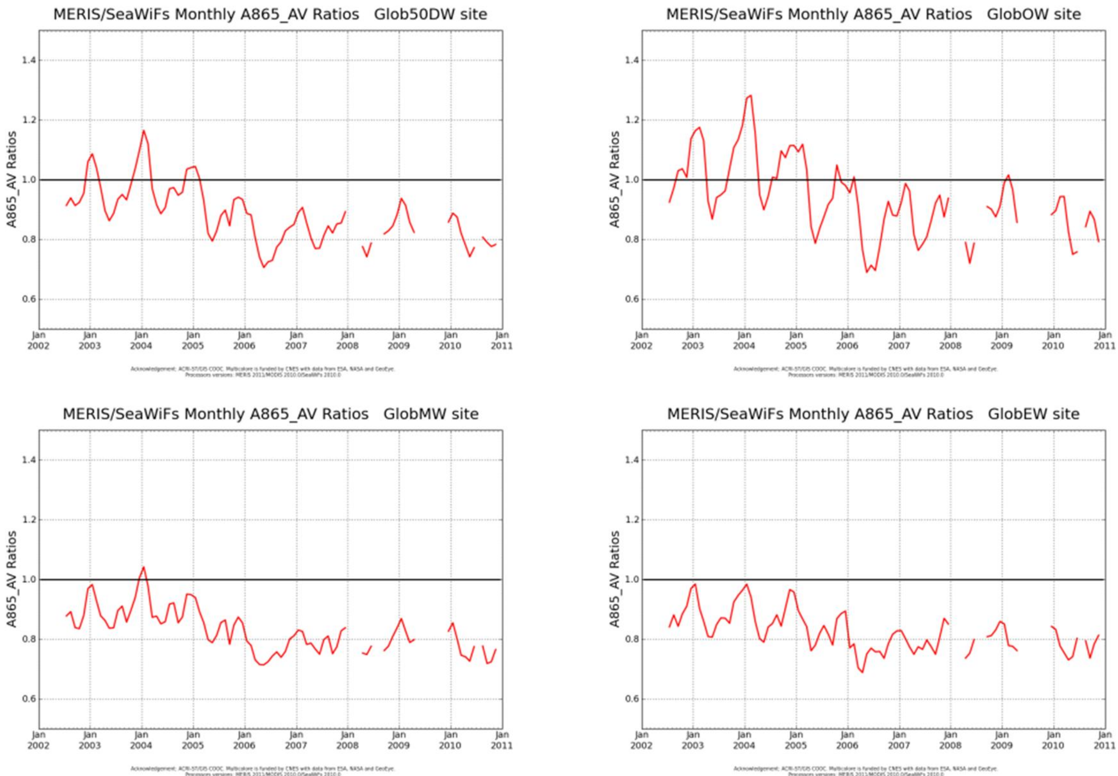

Figure 21: Monthly MERIS/SeaWiFS ratio time series for Deep water ocean (Glob50DW ; depth < 1000 m – latitude > 50°), Oligotrophic ocean (GlobOW ; chl < 0.1 mg.m^{-3}), mesotrophic ocean (GlobMW ; 0.1 < chl < 1.0 mg.m^{-3}) and eutrophic ocean (GlobEW ; 1.0 < chl < 10.0 mg.m^{-3})

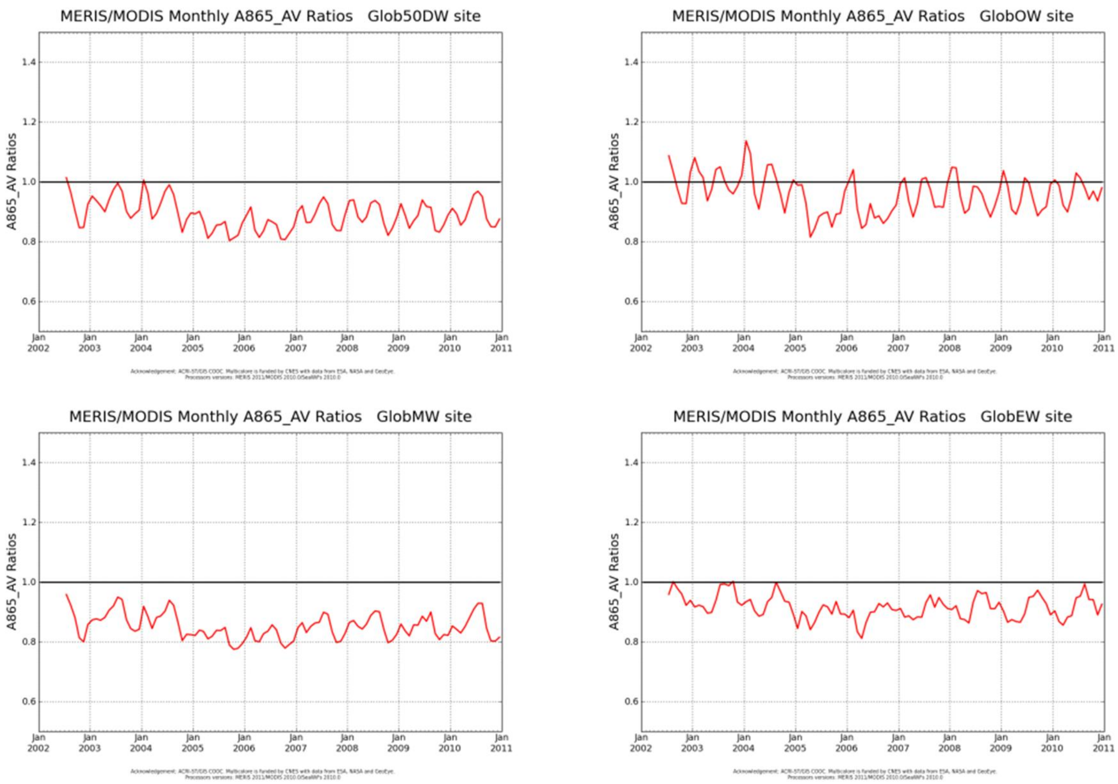

Figure 22: Monthly MERIS/MODIS ratio time series for Deep water ocean (Glob50DW ; depth < 1000 m – latitude > 50°), Oligotrophic ocean (GlobOW ; chl < 0.1 mg.m^{-3}), mesotrophic ocean (GlobMW ; 0.1 < chl < 1.0 mg.m^{-3}) and eutrophic ocean (GlobEW ; 1.0 < chl < 10.0 mg.m^{-3})

References

MERIS 3rd reprocessing, software update, 2011, ESA report, Ref A879.NT.008.ACRI-ST

Acknowledgement to the MERMAID team and PIs: G. Zibordi (AAOT, Abu Al Bukhoosh, Gloria, GustavDalenTower, HelsinkiLighthouse), G. Schuster & B. Holben (CoveSEAPRISM), V. Brando (LJCO), H. Feng & H. Sosik (MVCO), S. Kratzer (Palgrunden).

3.2 Cloud Products

3.2.1 Cloud Top Pressure

Parameter	Product type	Impacted by 3rd reprocessing	Contributor
Cloud-top pressure	☐ Ocean product ☒ Cloud product ☐ Land product ☐ Surface classification ☐ Product confidence ☐ Science flag	Yes : ☒ No : ☐	Dr. Rasmus Lindstrot (FUB) Dr. Rene Preusker (FUB) Prof. Jürgen Fischer (FUB)

Accuracy goal	Estimated quality
	Precision of 30hPa for low clouds, potential overestimation of cloud top-pressure for high clouds.

Method

The FUB algorithm for the retrieval of cloud-top pressure from MERIS measurements (CTP_{FUB}) was validated using airborne LIDAR measurements. The validation campaign was limited to low clouds over Germany.

Validation results

Due to the absence of validation data such as synchronous satellite-borne LIDAR measurement of cloud-top height, the only source for validation is an airborne LIDAR campaign, conducted by Lindstrot *et al.* (2006) in Northeastern Germany in 2004. Since the validation campaign was limited to low clouds (below 3km), no provable statement can be made for high and/or overlapping clouds. Few comparisons to A-train data seem to indicate a systematic overestimation of cloud-top pressure (underestimation of cloud-top height) by MERIS in cases of high clouds.

The airborne LIDAR campaign generally revealed a high accuracy of MERIS CTP for low, single-layer clouds. Figure 23 shows the comparison of CTP_{MERIS} and CTP_{LIDAR} for one exemplary day with homogeneous stratocumulus clouds. Except for a slight overestimation of cloud-top height, the MERIS-derived height closely follows the LIDAR observations. Further validation scenes showing similar results can be found in Lindstrot *et al*. (2006).

The summary of the complete validation campaign is shown in Figure 24. If cases with contamination by cirrus clouds are excluded (grey crosses), a RMSE of 25 hPa and a bias of 23hPa are found.

The MERIS CTP retrieval is based on O2A band radiances that are corrected for instrumental stray light. Due to uncertainties in the spectral calibration of the MERIS oxygen A band channel and improper corrections of instrumental stray light, the derived pressure products exhibit strong biases and jumps at the MERIS camera boundaries, if not corrected for these effects. An empirical stray light correction was developed by Lindstrot *et al*. (2010), which is applied to both the surface pressure as well as the cloud-top pressure retrieval. The camera effects are significantly reduced, however, locally still discontinuities of up to 40hPa in CTP can occur at the camera boundaries.

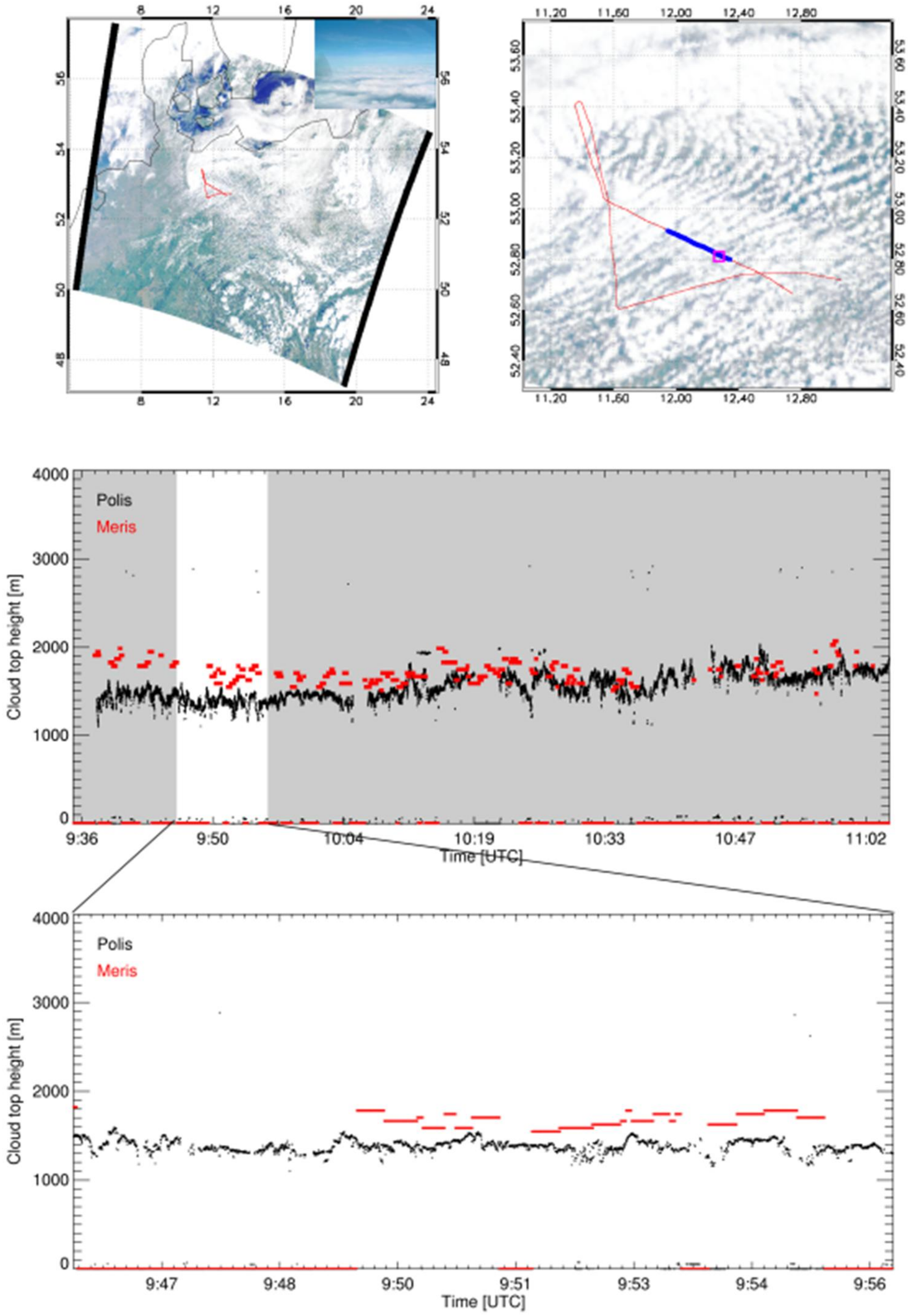

Figure 23: Comparison of MERIS- and LIDAR-derived cloud-top heights. The upper panels show the flight track of the aircraft, plotted over the MERIS RGB. The middle panel shows the comparison of both datasets for the complete measurements on that day, the overpass time of ENVISAT is indicated by the white background. The bottom panel shows a zoom into the overpass time ±5minutes. LIDAR measurements are shown in black, MERIS measurements are shown in red.

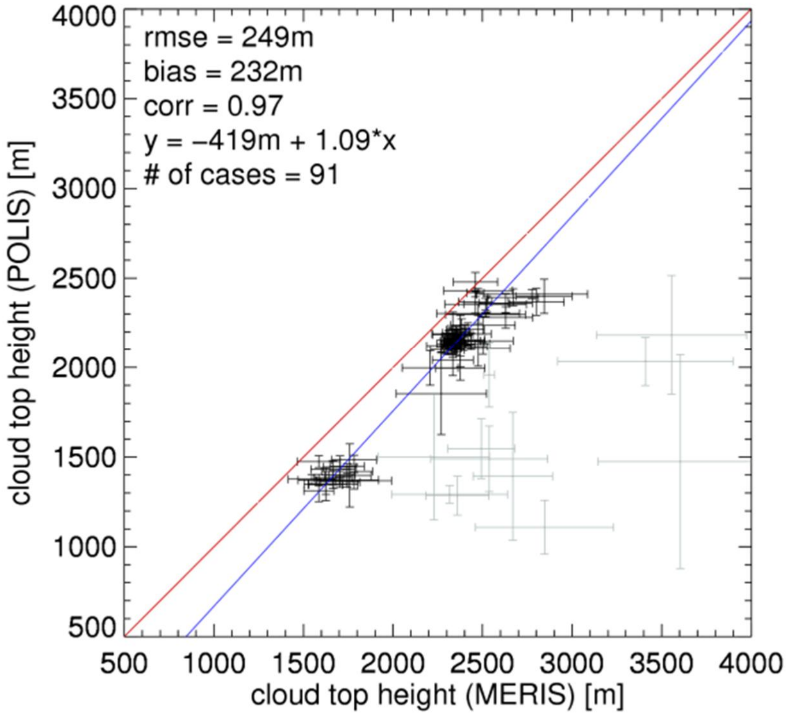

Figure 24: Scatter plot of MERIS- and LIDAR-derived cloud-top heights for the complete validation campaign. Grey crosses indicate cases with cirrus contamination and were not included in the analysis.

References

Lindstrot, R., R. Preusker, T. Ruhtz, B. Heese, M. Wiegner, C. Lindemann, and J. Fischer, 2006: Validation of MERIS Cloud-Top Pressure Using Airborne Lidar Measurements. *J. Appl. Meteor. Climatol.*, 45, 1612–1621.

Lindstrot, R., Preusker, R. and Fischer, J., 2010: The empirical correction of stray light in the MERIS oxygen A band channel, *J. Atmos. Oceanic Technol., 27 (7), 1185-1194.*

3.3 Land Products

3.3.1 MGVI/FAPAR

Parameter	Product type	Impacted by 3rd reprocessing	Contributor
MGVI/FAPAR Rectified Channels	☐ Ocean product ☐ Cloud product ☒ Land product ☐ Surface classification ☐ Product confidence ☐ Science flag	Yes : ☒ No : ☐	Nadine Gobron (EC-JRC)

Accuracy goal	Estimated quality
▪ MGVI: The accuracy goal of MGVI is set to -/+ 0.05 against FAPAR estimated by radiative transfer model. When comparing to interception ground-based estimates, the goal is -/+ 0.1 ▪ Rectified Channels: As these numbers are not 'measurable' parameters, the stability over long times is set to 5%.	▪ MGVI: The estimated quality is -/+0.1 in average when comparing with ground-based estimates. However, this value depends on the radiative transfer regime over various land cover sites. The algorithm is designed with the 'green leaf' concept and delivers instantaneous FAPAR values at time of overpass. ▪ Rectified Channels: The quality for the stability of rectified channel over

Method

The performance of the algorithm has been assessed using FAPAR products derived from additional sensors data, such as MODIS and SeaWIFS, using the same JRC algorithm.

Additional comparisons of MGVI values against few ground-based estimates of interception have been made over few sites of the BIGfoot project (Turner et al., 2005) and a site in Senegal (Fensholt et. al, 2004) following the comparison method published in Gobron et al. (2006, 2008).

The quality for the stability of rectified channels has been checked over CEOS desert calibration sites and compared with MODIS surface albedo.

Validation results

The performance of the algorithm has been assessed using FAPAR products derived from additional sensors data, such as MODIS and SeaWIFS, using the same JRC algorithm.

We found that the FAPAR derived from different sensors are in good agreement considering the variations in the angle of illumination (see Figure 25).

The accuracy, estimated against in-situ measurements is within -/+ 0.1 on average except for the senescence period as the 'green leaf' concept does not cope with the changing colour of leaves together with changing LAI (see Figure 26)

We found that daily MGVI is still contaminated by clouds but this undesired effect can be minimized using the JRC time-composite algorithm (Figure 26).

Note that the small differences from previous and new processing may be due to geo-location changes.

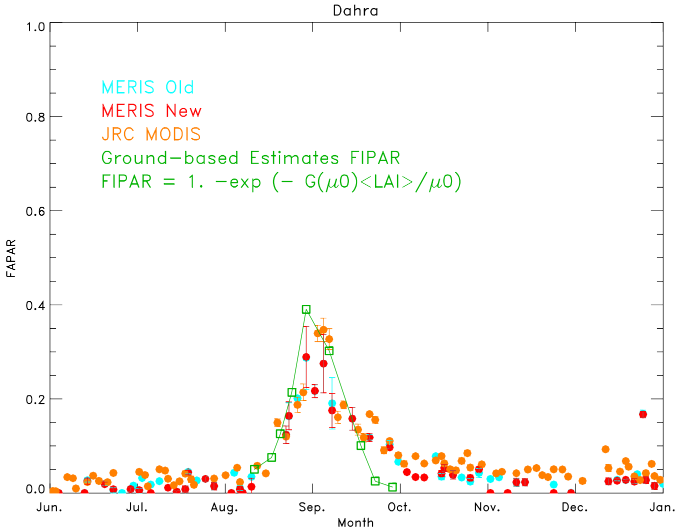

Figure 25 : Comparisons of ground-based FAPAR estimation profiles (empty green square symbols) and instantaneous daily MERIS FAPAR products (red full circle symbols) over the sites of Dahra North [15° 24′ N; 15° 26′ W associated with RT regime 1, i.e. for which the 1-D RT theory can be applied on the full domain. The blue and orange dotted points correspond to the previous processing MERIS data and MODIS derived products, respectively.

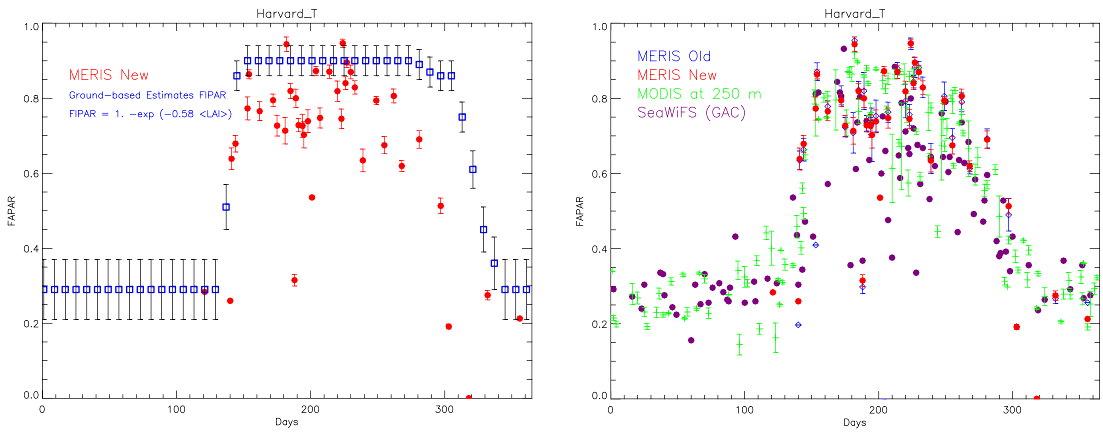

Figure 26 : Left panel: Comparisons of ground-based FAPAR estimation profiles (empty blue square symbols) and instantaneous daily MERIS FAPAR products (red full circle symbols) over Harvard site [42° 32′ N; 72° 10′ W] associated with RT regime 2, i.e. for which the 1-D RT theory can be applied on various land cover types of the domain and over the site. Right panel: The blue, red, green and purple dotted points correspond to previous and new processing MERIS data, MODIS and SeaWIFS derived products, respectively.

The stability of the two rectified channels over CEOS desert calibration site is estimated by computing the anomaly over long times period, for both SeaWiFS and MERIS, and we found -/+ 2 % of change in daily values (see Figure 27).

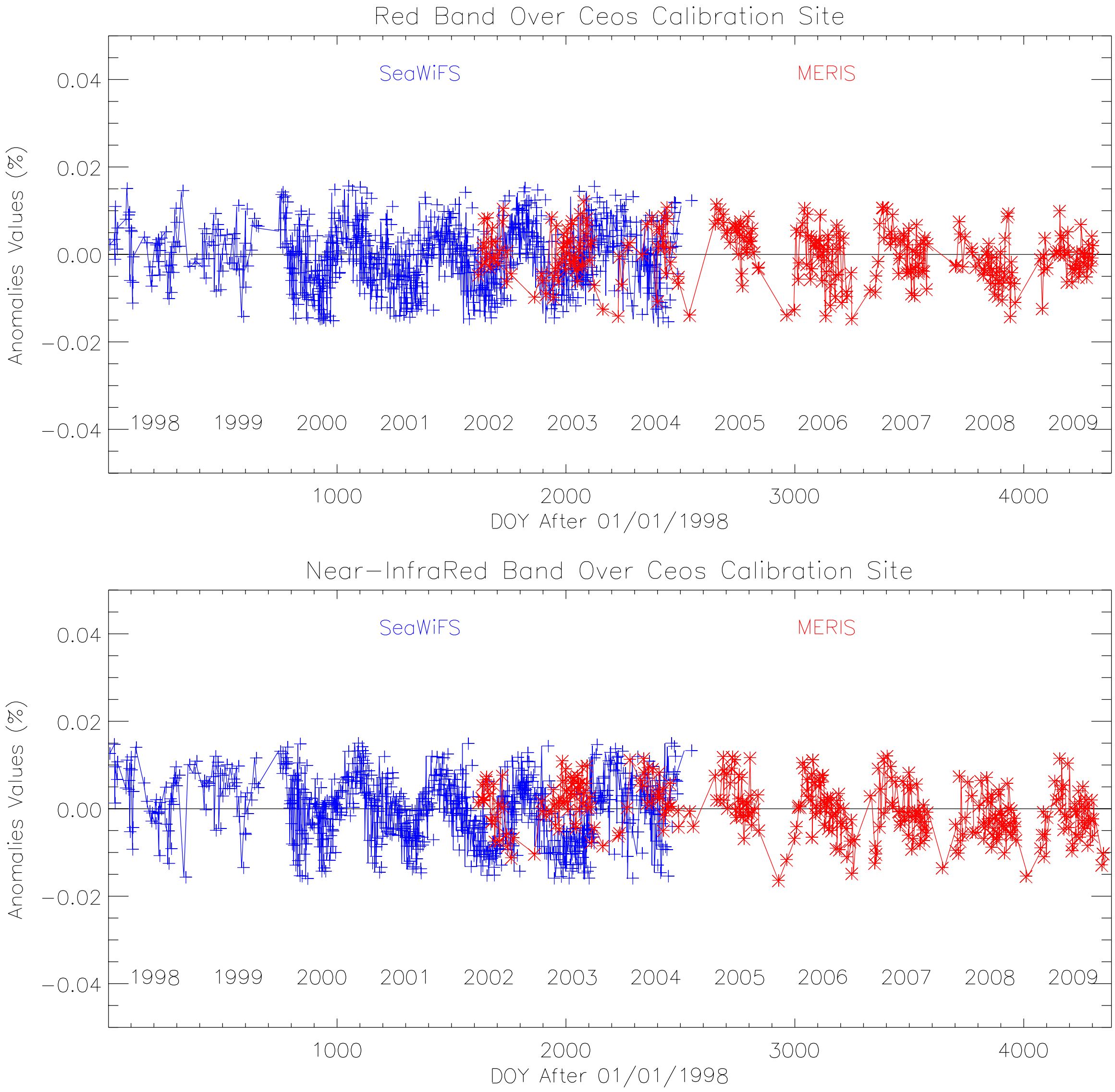

Figure 27 : Time series of daily rectified channels normalized by the average in the (top) red and (bottom) near-infrared spectral bands, respectively. Each data point corresponds to a spatial average over 15 × 15 pixels around the central pixel (28° 42′ 37″ N, 23° 18′ 59″ E) of a desert calibration site. The blue (red) line is for the SeaWiFS (MERIS) sensor, respectively.

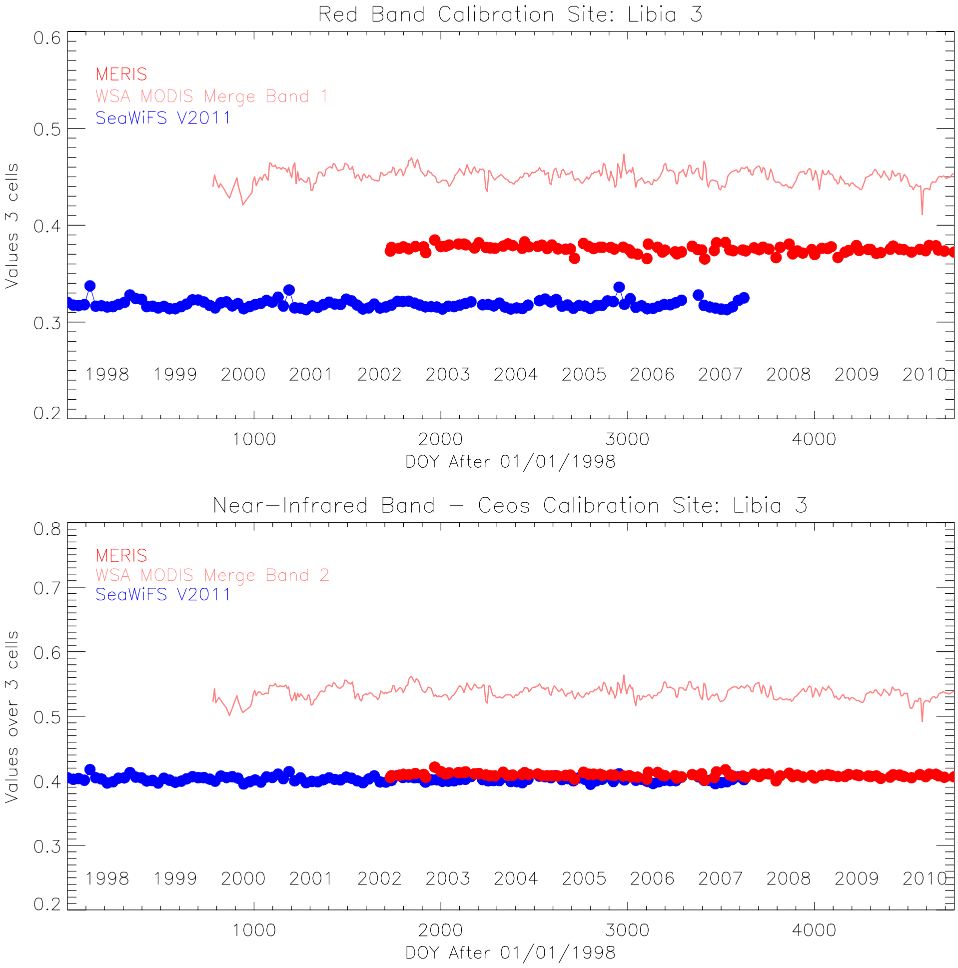

Figure 28 : Comparisons of rectified channels for SeaWiFS (blue dots) and MERIS (red dots) against white sky MODIS surface albedo (pink lines).

References

Gobron N., Pinty B., Aussedat O., Chen J. M., Cohen W. B., Fensholt R., Gond V., Lavergne T., Mélin F., Privette J. L., Sandholt I., Taberner M., Turner D. P., Verstraete M. M. and Widlowski J.-L. (2006) Evaluation of Fraction of Absorbed Photosynthetically Active Radiation Products for Different Canopy Radiation Transfer Regimes: Methodology and Results Using Joint Research Center Products Derived from SeaWiFS Against Ground-Based Estimations. Journal of Geophysical Research – Atmospheres, 111(D13110): 15 PP. DOI: 10.1029/2005JD006511

Gobron N., Pinty B., Aussedat O., Taberner M., Faber O., Mélin F., Lavergne T., Robustelli M. and Snoeij P. (2008) Uncertainty Estimates for the FAPAR Operational Products Derived from MERIS - Impact of Top-of-Atmosphere Radiance Uncertainties and Validation with Field Data. Remote Sensing of Environment, 112(4): 1871-1883. DOI: 10.1016/j.rse.2007.09.011

Gobron N., Belward A. S., Pinty B. and Knorr W. (2010) `Monitoring Biosphere Vegetation 1998-2009. Geophysical Research Letters, 37(L15402). DOI: 10.1029/2010GL043870

Turner, D. P., et al. (2005), Site-level evaluation of satellite-based global terrestrial gross primary production and net primary production monitoring, Global Change Biol., 11, 666–684.

Fensholt, R., I. Sandholt, and M. S. Rasmussen (2004), Evaluation of MODIS LAI, fAPAR and the relation between fAPAR and NDVI in a semi-arid environment using in situ measurements, Remote Sens. Environ., 91, 490–507.

3.3.2 MTCI

Parameter	Product type	Impacted by 3rd reprocessing	Contributor
MERIS Terrestrial Chlorophyll Index (MTCI) BOA Vegetation Index	☐ Ocean product ☐ Cloud product ☒ Land product ☐ Surface classification ☐ Product confidence ☐ Science flag	Yes : ☐ No : ☒	University of Southampton ▪ Dr. Jadunandan Dash ▪ Dr. Francesco Vuolo ▪ Dr. Gary Watmough ▪ William Frampton

Accuracy goal	Estimated quality
	Good

Method

The validation of satellite derived canopy chlorophyll content products, such as MTCI, is particularly challenging because the signal observed from satellite sensors integrates the effects of leaf biochemistry and canopy structure (i.e., foliage amount, spatial arrangement and leaf orientation). Moreover, it is influenced by the intercepted radiation from other elements such as non photosynthetic materials (branches, stems and shoots) and underlying soils. The “bottom-up” approach developed for validation of MTCI was based on the framework of the Land Product Validation (LPV) Subgroup of the CEOS Working Group on Calibration and Validation (http://lpvs.gsfc.nasa.gov/) and is at stage 1 of the validation cycle (validation using <30 locations and time period). The “bottom-up” starts with local field-level data and move towards global comparisons using satellite data. Validation of MTCI based on bottom-up approach consists of 3 steps (see figure below):

1. Field data collection: Both Leaf Area Index (LAI) and chlorophyll concentration were collected at a number of (more than 20) Elementary Sampling Units (ESU). Within each ESU, several individual LAI (generally using a LAI2000 instrument) and leaf chlorophyll concentration (generally using a SPAD) measurements were undertaken. The number and distribution of individual measurement depends on the site heterogeneity. Both LAI and leaf chlorophyll concentration are combined to provide the canopy chlorophyll content (g. m^{-2}) per ESU;

2. High spatial resolution remote sensing data processing: Airborne remote sensing data (such as those from CASI) or high spatial resolution space borne data with adequate spectral bands (such as Rapideye) can be used as an intermediate layers. These data were corrected for geometric and atmospheric effects and were then used to produce high spatial resolution canopy chlorophyll map. This is generally achieved by either model inversion or using empirical relationship with vegetation indices. The high spatial resolution canopy chlorophyll map was then validated with ESU;

3. Validation of MTCI: The high spatial resolution canopy chlorophyll map was then up-scaled to MERIS spatial resolution. Pixel wise comparison was made and the correlation coefficient between MTCI and canopy chlorophyll content were reported.

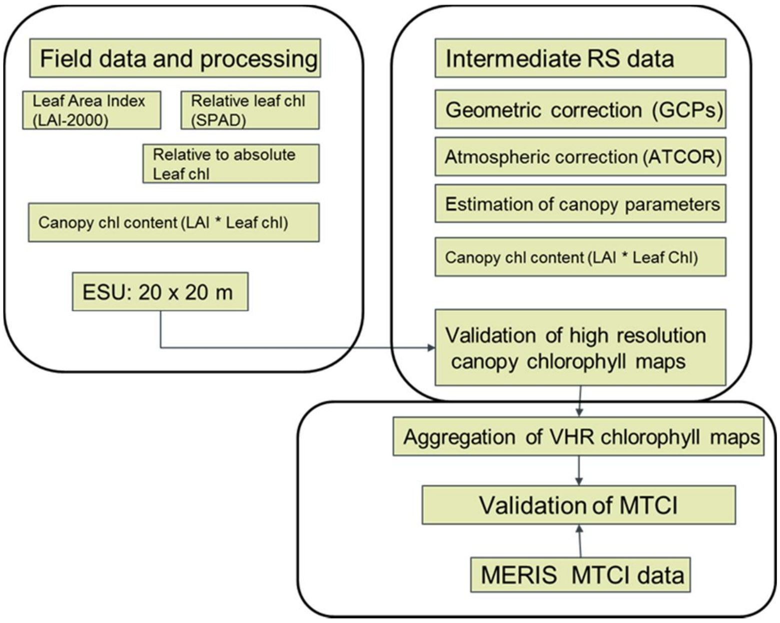

Figure 29 : Bottom-up approach validation procedure for MTCI

Validation results

Although MTCI has been validated for more than 5 sites, we present results from 2 sites here.

Validation results from New forest study site

The study site is situated in the New Forest National Park in southern England (0°56'N, 1°5'W). It covers approximately 9 km² of both ancient semi-natural woodlands and managed coniferous plantations and adjacent heathland. Ground chlorophyll concentration and LAI data were obtained for 31 sampling plots (20 m x 20 m) and these, in conjunction with CASI data were used to derive a high spatial resolution chlorophyll content map. This was aggregated to the spatial resolution of MERIS and then related to MTCI. There was a positive relationship between chlorophyll content and MTCI with coefficient of determination (R^2) 0.56 (Dash et al., 2008).

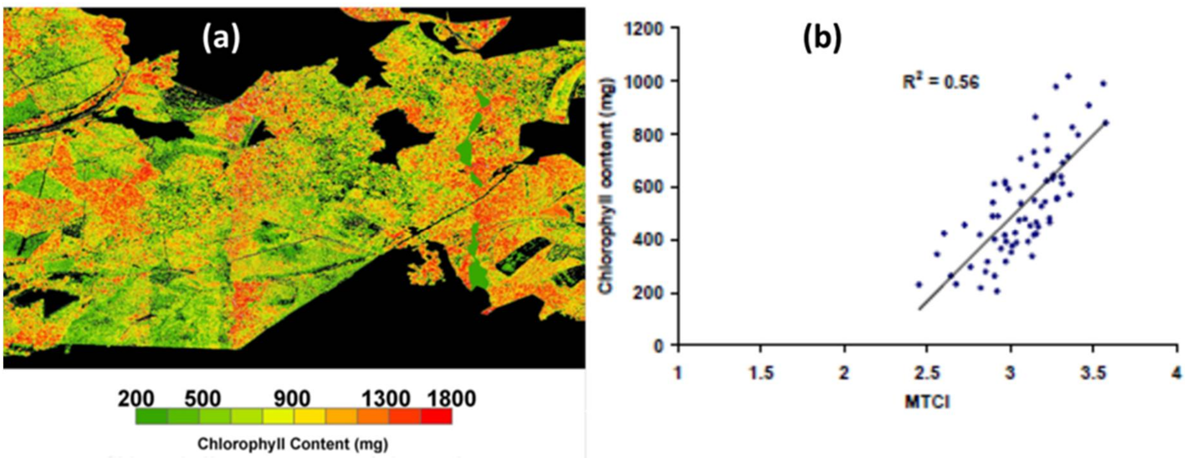

Figure 30 : (a) Chlorophyll content map of the study area derived from CASI data and ground data of chlorophyll content. Areas in black represent missing data or non-vegetated areas. (b) Relationship between MTCI and chlorophyll content for the study site at MERIS spatial resolution

Validation results from Campania region of Southern Italy

This study was undertaken at the 560 km² 'Piana del Sele' site in the Campania region of Southern Italy (40.52°N, 15.00°E). The study site, one of the largest agricultural areas in the region, is characterized by irrigated agriculture (mainly forages, fruit trees and vegetables) with an average field size of about 2 ha. LAI and leaf chlorophyll concentration were estimated using a random sampling scheme within each of 36 ESUs. Multispectral data were acquired on 17 August 2009 (at 10:35 UTC) from Choros, a satellite in the RapidEye constellation. Model inversion was used to produce a canopy chlorophyll map at RapidEye spatial resolution (6.5 m). Subsequently, this map was aggregated to medium spatial resolution based on a regular grid (1 km) to validate MERIS L2 MTCI. There was a strong positive relationship between MTCI and canopy chlorophyll content with coefficient of determination (R^2) 0.74. (Vuolo, 2012).

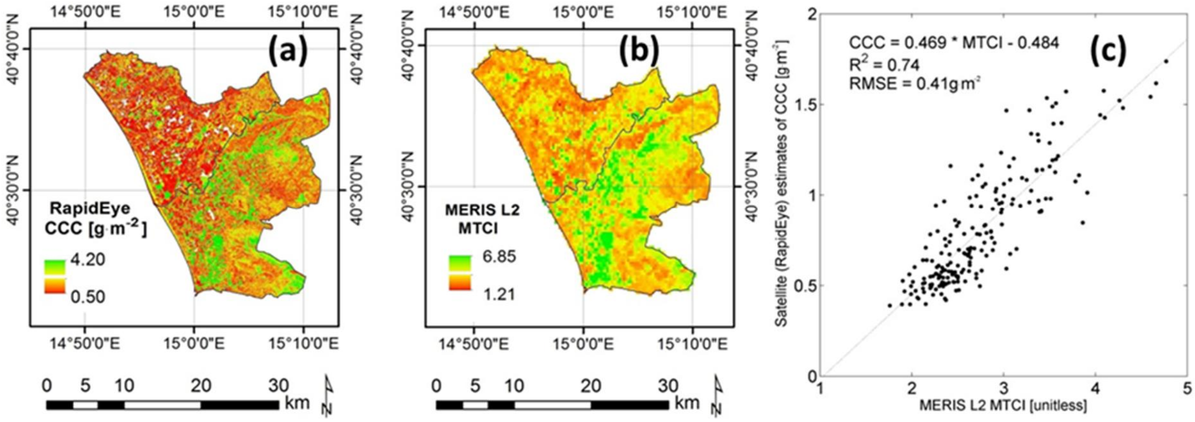

Figure 31 : (a) Fine spatial resolution canopy chlorophyll content [g.m^{-2}] map from RapidEye satellite sensor data and (b) medium spatial resolution MERIS L2 MTCI data. The two maps were aggregated and compared at 1 km spatial resolution based on the position of MERIS pixels. (c) Relationship between MTCI and chlorophyll content for the study site at 1 km spatial resolution.

References

Dash, J., Boyd, D., Almond, S. and Curran, P. J., 2008, Multi-scale analysis and validation of the Envisat MERIS Terrestrial Chlorophyll Index (MTCI) in woodland, Proceedings of the 2nd MERIS/ (A)ATSR workshop, Frascati, Rome, Italy, 22-26 September 2008, (ESA SP-666)(CD Rom).

Vuolo, F., Dash, J., Curran, P. J., Lajas, D. and Kwiatkowska, E., 2012, Methodologies and uncertainties in the use of the Terrestrial Chlorophyll Index for the Sentinel-3 mission, Remote Sensing, 4; doi:10.3390/rs40x000x

Dash, J. and Curran, P. J., 2004, The MERIS Terrestrial Chlorophyll Index. International Journal of Remote Sensing, 25, pp-5003-5013.

3.3.3 Aerosol Optical Thickness and Angström Coefficient

Parameter	Product type	Impacted by 3rd reprocessing	Contributor
Aerosol Optical Thickness (or Depth) at 443 nm, 550 nm & Angström exponent over land	☐ Ocean product ☐ Cloud product ☒ Land product ☐ Surface classification ☐ Product confidence ☐ Science flag	Yes : ☒ No : ☐	D. Ramon (HYGEOS) Contribution of the ESA CCI aerosol project

Accuracy goal	Estimated quality
Standard published accuracy of aerosol products over land (i.e. MODIS) : AOT(443, 550 nm)=0.05 + 0.15* AOT	AOD at 443 nm Validation against AERONET matchups: ▪ (March, June, Sept., Dec. 2008) MEGS 8.0: N=836, r^2=0.609, RMSE=0.180, Gfrac=0.37 ✓ (filtered, *(AOD) <0.1): N=770, r^2=0.664, RMSE=0.17, Gfrac=0.39 ✓ Variability: June 2003 Gfrac=0.52, June 2008 Gfrac=0.29, Dec. 2008 Gfrac=0.61 ▪ (2004-2010) MODIS coll. 5: N=5448, r2=0.871, rmse=0.137, Gfrac=0.62 (Breon *et al.*, 2011) Angström coefficient The Angström exponent over land is not validated and poorly correlated to AERONET.

Method

- Comparison to AERONET spectral Aerosol Optical Depth measurements at 443 and 550 nm and Angström exponent between 443 and 675 nm. AERONET data within +/-15 minutes are averaged and compared to MERIS 10x10km box averaged aerosol products where no pixel is flagged as cloud. March, June, September and December 2008 are considered, globally.
- Comparison to MODIS Aqua global monthly AOD 550 dataset

Validation results

The aerosol product over land is at the same resolution that the L1 product (i.e. at 1.2 km in Reduced Resolution mode). Could contamination is the main issue and induces a large positive bias on AOD (see Figure 32a). The improvement of the cloud masking between 2nd and 3rd reprocessing reduced a bit this contamination but it is not yet satisfactory. Removing some outliers in a 10 x 10 box with a test on spatial variance of the AOD (see Figure 32b or see Vidot et al. 2008 for the 2nd reprocessing product validation results) is a slight improvement yielding a fraction of good retrieval Gfrac (as defined by Bréon et al., 2011) of 39% for AOD at 443 nm for 4 months in 2008. However, seasonal variability of the retrieval accuracy is important, Gfrac varying from 29% in June 2008 to 61% in December 2008.

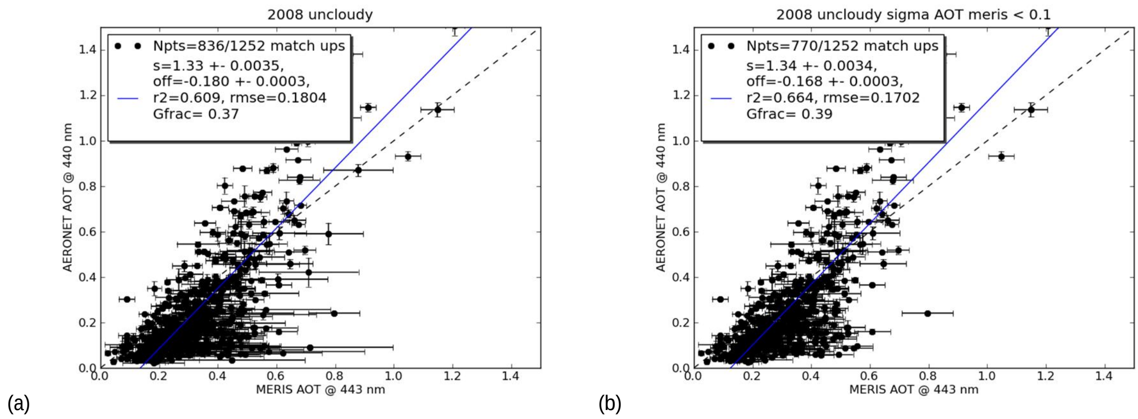

Figure 32: Comparison a of daily 10 km averaged AOD at 443 nm over land from MERIS 3rd reprocessing and AEONET AOD for 4 months of 2008. (a) Original dataset with macro pixels free of cloudy flagged pixels; (b) Same as (a) but where the macro pixels with a spatial standard deviation of AOD greater than 0.1 have been discarded

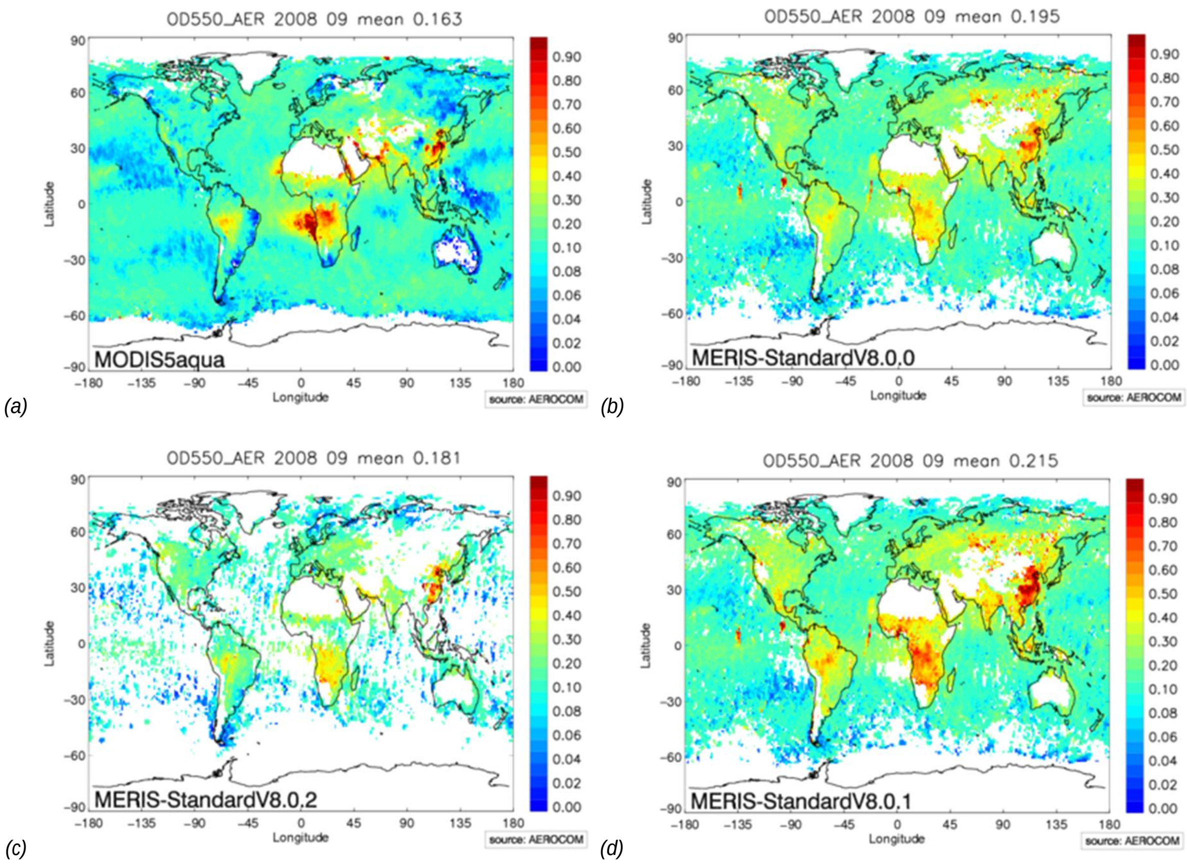

Figure 33: Monthly mean of AOD at 550 nm for the month of September 2008 on a 1°x1° grid. a) MODIS Aqua b) MEGS 8.0 and c) MEGS 8.0 with the AATSR cloud mask applied to MERIS and d) MEGS 8.0 with a posteriori corrections using a realistic aerosol model climatology (from the AEROCOM project)

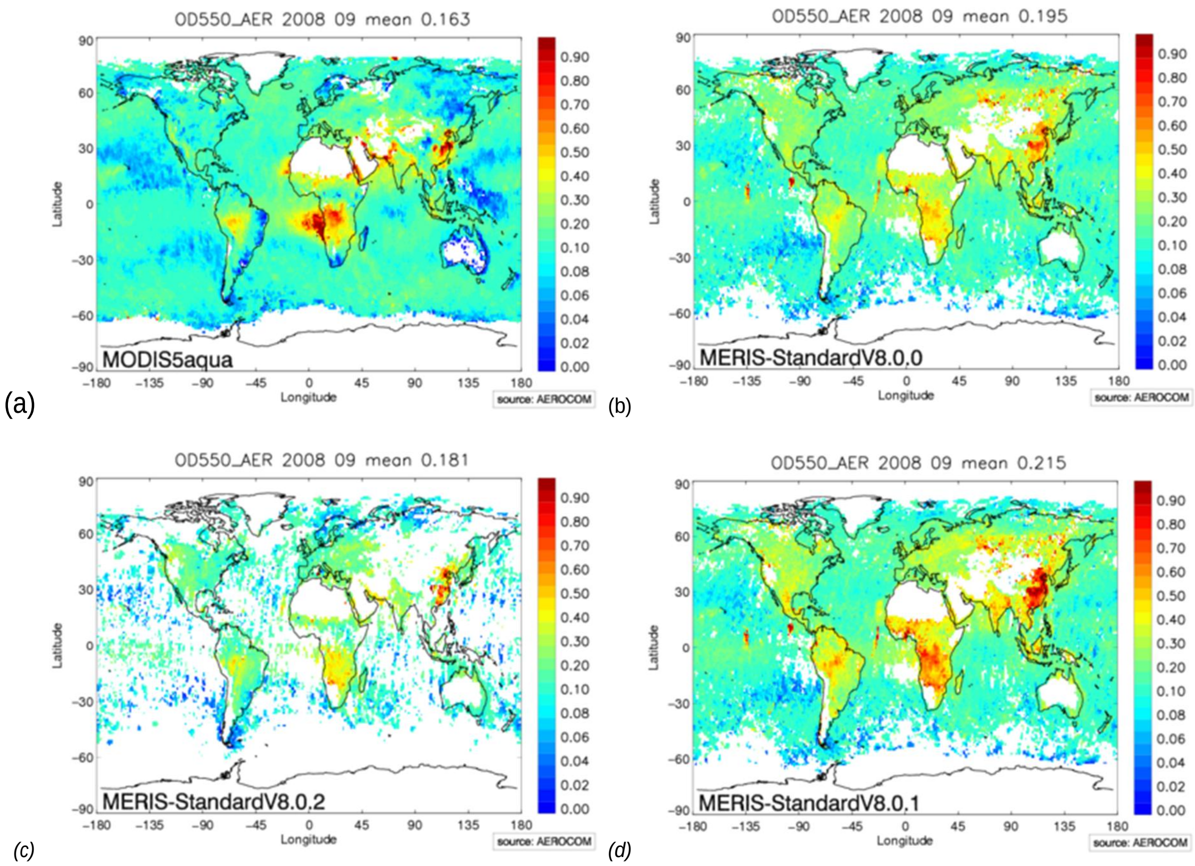

Figure 33 shows a monthly synthesis of the AOD product at 550 nm for September 2008. Compared to MODIS, areas with large cloud contaminations are clearly identified. Biomass burning aerosols in Africa and urban/industrial pollution aerosol in East Asia are underestimated. Both issues seems to be at least partly resolved if we use an external robust cloud mask (here from AATSR) and an improved aerosol model climatology (here from AEROCOM). This was also a recommendation of Vidot et al. 2008.

References

CCI Aerosol project: Validation Report, To be published (http://www.esa-aerosol-cci.org)

Vidot, J., R. Santer, and O. Aznay, Evaluation of the MERIS aerosol product over land with AERONET, Atmospheric Chemistry and Physics, 8, 24 7603-7617 (2008)

Bréon F.-M., A. Vermeulen and J. Descloitres, An evaluation of satellite aerosol products against sunphotometer measurements, Remote Sensing of Environment, Volume 115, Issue 12, 3102-3111 (2011)

3.3.4 Surface Pressure

Parameter	Product type	Impacted by 3rd reprocessing	Contributor
Surface pressure	☐ Ocean product ☐ Cloud product ☒ Land product ☐ Surface classification ☐ Product confidence ☐ Science flag	Yes : ☒ No : ☐	Dr. Rasmus Lindstrot (FUB) Dr. Rene Preusker (FUB) Prof. Jürgen Fischer (FUB)

Accuracy goal	Estimated quality
	Precision of 15hPa, no bias in mid latitudes, positive bias (≤25hPa) in high latitudes, negative bias (≤25hPa) in tropics.

Method

The FUB algorithm for the retrieval of surface pressure from MERIS measurements (SP_{FUB}) was compared to surface pressure maps derived from digital elevation models, corrected for the variable sea level pressure (extracted from ECMWF). In order to prove the correct implementation of the algorithm in the MERIS ground segment, the FUB breadboard algorithm was applied to several L1B scenes (3rd reprocessing) and compared to the L2 data.

Validation results

The algorithm for the retrieval of surface pressure from MERIS measurements is based on the assumption of a globally fixed US standard temperature profile. Due to the temperature- and pressure-broadening of the individual absorption lines, the strength of the oxygen absorption is a function of the temperature profile. Consequently, a bias of up to ± 25hPa is found wherever the actual atmospheric profile deviates from the US standard profile, with negative biases occurring where the actual profile is warmer and vice versa.

Apart from this effect, SPFUB shows a precision of 15hPa, when compared to surface pressure derived from digital elevation models (SPDEM). Figure 34 and Figure 35 show a comparison of SPFUB and SPDEM for a desert scene (Libyan desert). There is no bias, since the SPFUB version shown here was trained assuming a tropical temperature profile, while it is similar to the US standard version in all other aspects.

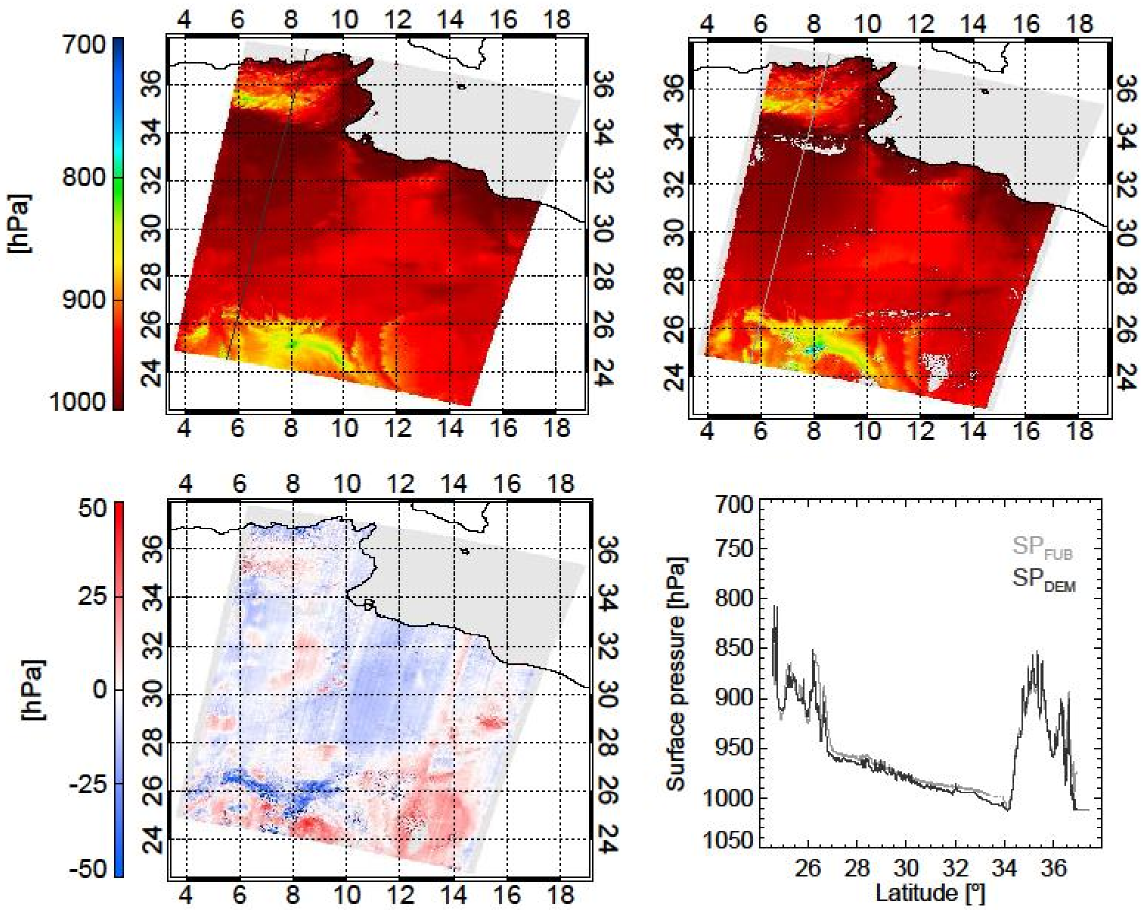

Figure 34: Comparison of SP_{DEM} (top left) and SP_{FUB} (top right) for Libyan desert scene. Difference of both is shown in bottom left panel, section plot along line indicated in upper panels is shown in bottom right panel.

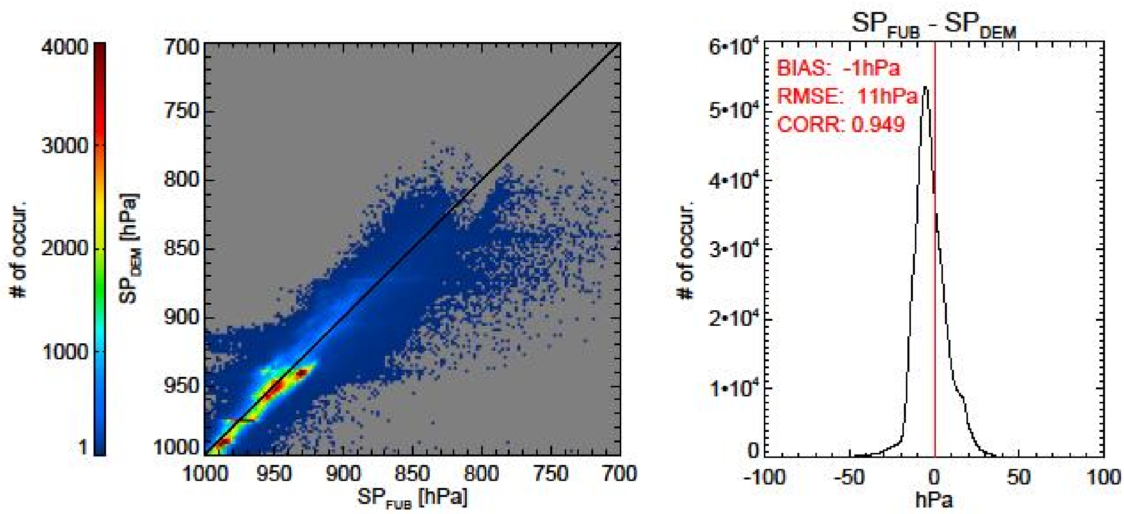

Figure 35: Histograms of SP_{FUB} and SP_{DEM} comparison for scene shown in Figure 34

Further validation scenes showing similar results can be found in Lindstrot et al. 2009.

The results shown are, like the operational L2 product, corrected for instrumental stray light. Due to uncertainties in the spectral calibration of the MERIS oxygen A band channel and improper corrections of instrumental stray light, the derived surface pressure exhibits a strong bias and jumps at the MERIS camera boundaries, if not corrected for these effects. An empirical stray light correction was developed by Lindstrot et al (2010), which is applied to both the surface pressure as well as the cloud-top pressure retrieval. The camera effects are significantly reduced, however, locally still discontinuities of up to 20hPa can occur at the camera boundaries.

Figure 36 shows a comparison of the in-house algorithm SP_{FUB}, applied to 3rd reprocessing L1b data, with the operational L2 algorithm results for one exemplary MERIS orbit. The scatter plot shows that both retrievals perfectly agree with a root mean square deviation of 1hPa and no bias.

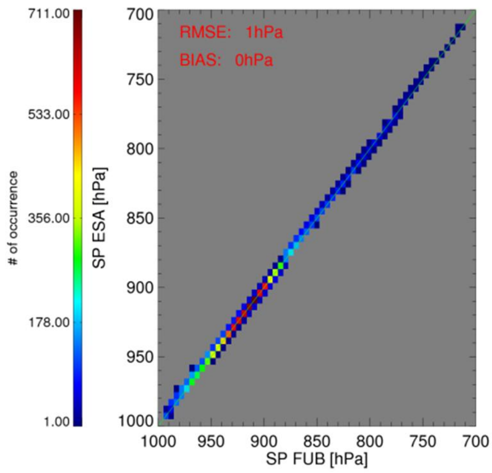

Figure 36: Comparison of SP_{FUB} and SP_{ESA} for one exemplary orbit

References

Lindstrot, R, Preusker, R. and Fischer, J., 2009: The retrieval of land surface pressure from MERIS measurements in the oxygen *A* band, *J. Atmos. Oceanic Technol.,* 26 (7), 1367–1377.

Lindstrot, R., Preusker, R. and Fischer, J., 2010: The empirical correction of stray light in the MERIS oxygen A band channel, *J. Atmos. Oceanic Technol., 27 (7), 1185-1194.*

3.3.5 Total Column Water Vapour

Parameter	Product type	Impacted by 3rd reprocessing	Contributors
Total Column Water Vapour (TCWV)	☐ Ocean product ☐ Cloud product ☒ Land product ☐ Surface classification ☐ Product confidence ☐ Science flag	Yes : ☒ No : ☐	Prof. Jürgen Fischer (FUB) Ronny Leinweber Hannes Diedrich

Accuracy goal	Estimated quality
	Precision of 2 mm for cloud-free pixels for different reference datasets.

Method

The in-house total column water vapour (TCWV) algorithm was already validated with *in-situ* data such as GPS and microwave radiometer measurements (Fischer et al., 2010). The agreement between *in-situ* data and the MERIS-algorithm, based on an artificial neuronal network (ANN), is very good within the analysed period between 2003 and 2005. The root mean square errors (RMSE) of the comparison datasets are in the range of the measurement accuracy. This result shows the high accuracy of the algorithm, which justifies its use as a comparison-method.

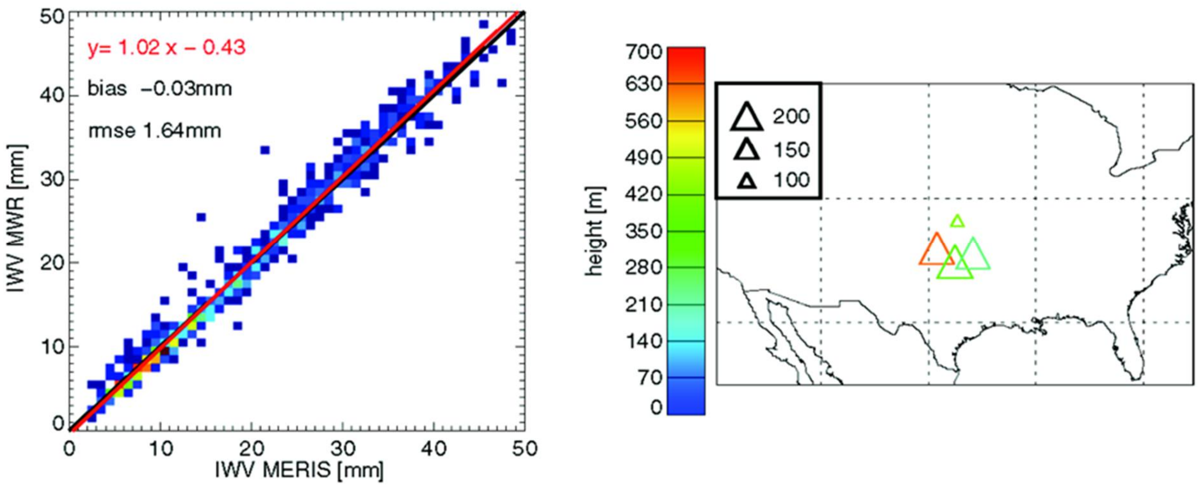

Figure 37: Integrated water vapour from MERIS and Microwave Radiometer at ARM-SGP site. The upper left panel shows the scatter-plot of 794 collocations for a period of three years. The colour indicates the number of collocations with high values in red and small values in blue. The right panel illustrates the location of the four used microwave radiometer stations. The size of the triangles denotes the number of observations used for the comparison, while the colour indicates the height of the MWR-station (Fischer et al., 2010).

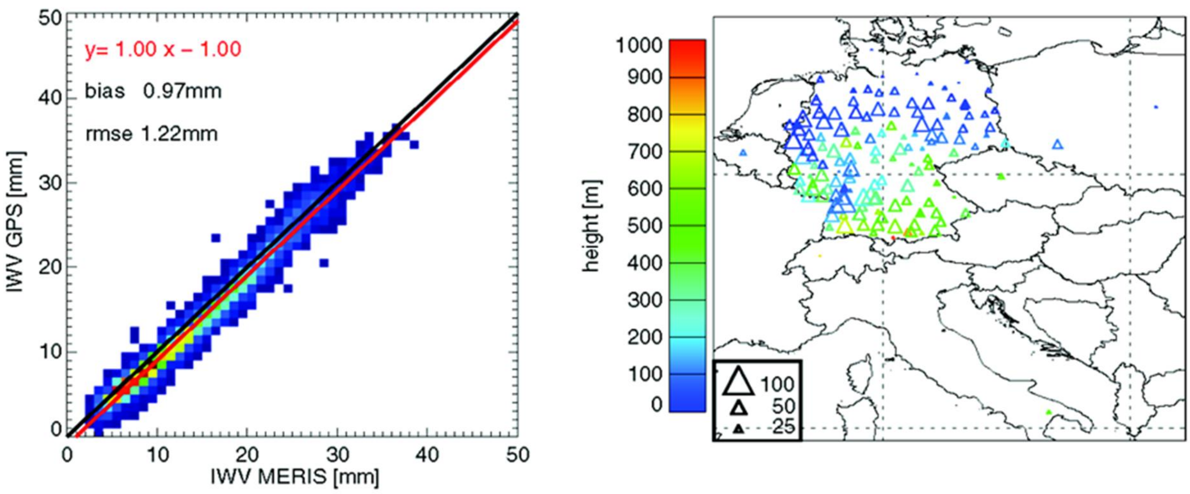

Figure 38: Integrated water vapour from MERIS and from GPS measurements located in Central Europe. The upper left panel shows the scatterplot of 4424 collocations for a period of three years. The colour indicates the number of collocations with high values in red and small values in blue. The right panel illustrates the location of the four used microwave radiometer stations. The size of the triangles denotes the number of observations used for the comparison, while the colour indicates the height of the GPS-station [Fischer, 2010].

Validation results

For validation of the TCWV product we retrieved the TCWV from L1-MERIS-RR-data with the in-house algorithm and compared to the 3rd-reprocessed-L2-TCWV values for four subsets of data. Exemplarily one subset was chosen for presentation.

In Figure 39 the scatterplot of all TCWV values for all cloud-free land-pixels from a scene, captured over south-east Asia on the 2008-04-10 at 03:02 UTC, is shown. The corresponding difference-plot is presented in Figure 40. The agreement between both datasets is very good. The RMSE is in the range of uncertainty of the in-house algorithm (see Figure 37 and Figure 38).

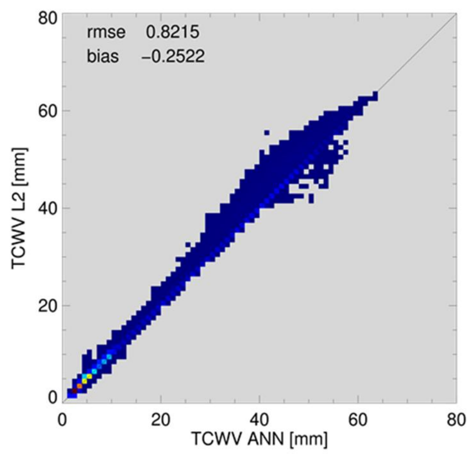

Figure 39: Scatterplot of TCWV from L2 reprocessed data and in-house-algorithm (ANN) in mm. Red pixel account for high and blue for low density of colocations between the two methods.

On the one hand the maximum difference between both datasets is 2 mm. On the other hand the majority of TCWV-values is equal (see Figure 40).

An explanation for the scattering and the small bias can be the use of different methods to determine the surface albedo in the absorption channel at 900 nm. For the in-house algorithm linear interpolation between the window channels (865 and 885 nm) was applied to determine the spectral slope of the surface albedo.

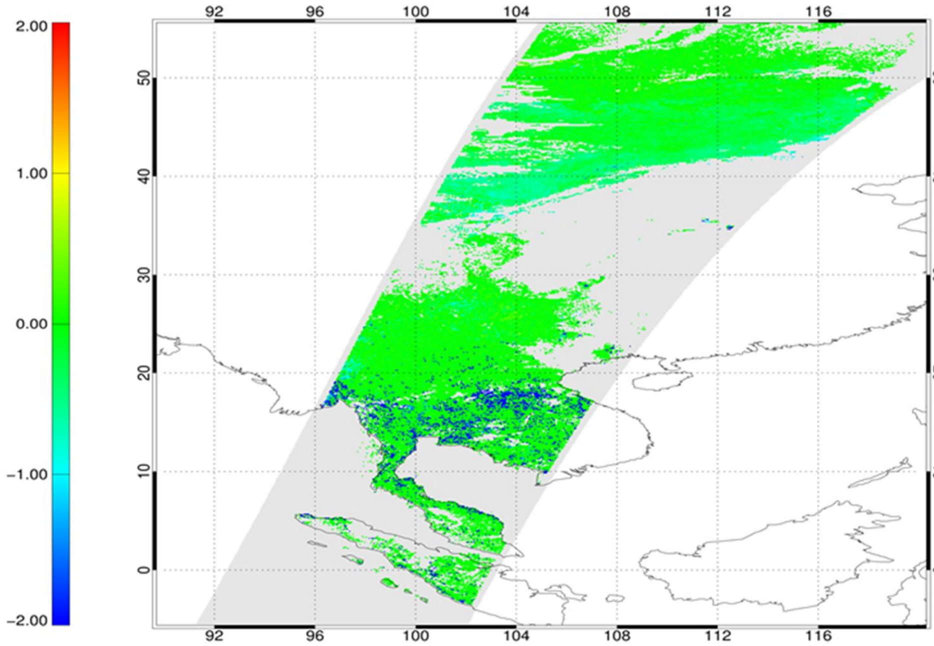

Figure 40: Difference between TCWV from L2-reprocessed-data and in-house algorithm (ANN) in mm.

References

J. Fischer, R. Leinweber, R. Preusker: MERIS ATBD 2.4: Retrieval of Total Water Vapour Content from MERIS Measurements, ESA, ESRIN, 2010.

3.4 Surface Classification

Parameter	Product type	Impacted by 3rd reprocessing	Contributor
Flags	☐ Ocean product ☐ Cloud product ☐ Land product ☒ Surface classification ☐ Product confidence ☐ Science flag	Yes : ☒ No : ☐	▪ K. Stelzer (BC) ▪ A. Ruescas (BC) ▪ C. Brockmann (BC) ▪ M. Paperin (BC)

Accuracy goal	Estimated quality
95%	73.5% – 99.5%

Method

The validation of the pixel classification has been performed with the PixBox Dataset. The PixBox dataset is a hand-selected dataset of 110,000 MERIS RR pixels and 40,000 MERIS FR pixels which have been classified visually into different surface classes by an expert. The classes cover different cloud classes, clear land/water pixels, snow and ice pixels as well as mixed pixels of different surface types. This dataset has been tested against the flagging of the L2 3rd reprocessing products for assessing the quality of the cloud flag. The results are presented in a contingency matrix. Further, selected scenes are investigated visually how the pixel classification is working.

Validation results

PixBox results RR

The outcome of the PixBox validation is a confusion matrix indicating the correctly flagged pixels shown in Figure 41. A total number of 57,264 pixels are used within this comparison, which is a subset of total pixels because this matrix is showing only the "clear cases". The diagonal line show the matching pixels between PixBox categorisation and L2_flagging.

L2_Flag / PixBox	WATER	CLOUD	LAND	Σ	%
clear water	6875	1065	757	9319	73.5
cloud	61	31296	104	31461	99.5
land	85	957	15419	16484	93.5
Σ	7021	33318	16925	57264	
%	97.6	93.9	91.1		93.5

Figure 41: Confusion matrix of PixBox investigation of MERIS RR for the flags/classes clear water, cloud, land.

Pixels that are not on the diagonal can be mainly explained by:

- The 757 pixels that are flagged as LAND but classified in PixBox as clear water are due to uncertainties in the land-water mask. 91% of these pixels are lake pixels, which were not included in the L2_water flag or where the flag is shifted.
- The 1065 pixels that are flagged as CLOUD but classified in PixBox as clear water are mainly due to glint (71%) or highly turbid water (18%).
- The 85 pixels that are flagged as WATER but classified in PixBox as land are mainly due to cloud shadow. This effect occurs when the spectral test is performed and the cloud shadow indicates that there are very dark pixels, similar to water spectra.

Investigations have been performed also on mixed pixels such as semi-transparent clouds or mixed land/cloud; water/cloud pixels. Mixed pixels over water are flagged in 30% of the cases as WATER, while 70% are flagged as CLOUD. Over land surfaces, mixed pixels are flagged in 70% as LAND and 30% as CLOUD.

PixBox results FR (over land only)

Figure 42 shows the confusion matrix for MERIS for pixel classification, where at the moment only pixels over land are included. The percentage of matching clear pixels is over 97%, except for snow/ice surfaces, which show an agreement of 91.8%.

L2_Flag / PixBox	ICE-SNOW	CLOUD	LAND*	Σ	%
snow	466	434	9	909	51.3
cloud	31	5999	38	6068	98.9
land	1	245	4667	4913	95.0
Σ	498	6678	4714	11890	
%	93.6	89.8	99.0		93.6
			*clear sky, no snow		

*Figure 42: Confusion matrix of PixBox investigation of MERIS FR for the flags/classes clear ice-snow, cloud and land (* clear sky, no snow)*

The outcome of the investigation of mixed pixels within the FR data is that 28% of the mixed pixels are flagged as CLOUD, while 72% are flagged as LAND. This includes semi-transparent clouds over land and mixed cloud/land pixels. In total 2940 mixed pixels have been analysed.

Investigation of selected scenes

The figures below show some examples of the performance of the cloud classification on L2 Reduced Resolution and Full Resolution scenes.

Good classification of the different surfaces in L2 RR (MER_RR__2PNACR20070102_075728)

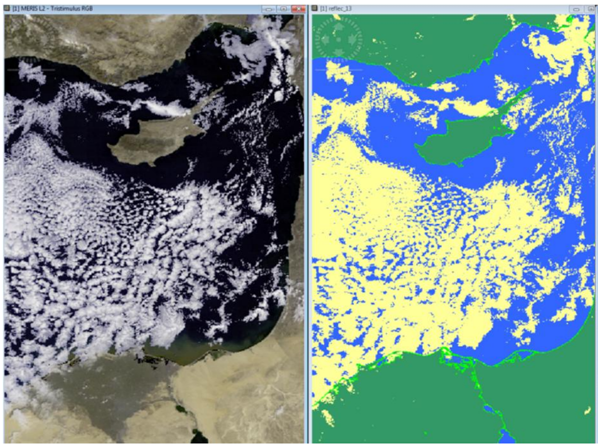

Misclassification of cirrus and small patchy clouds over land in L2 RR (MER_RR__2PNACR20070128_160142)

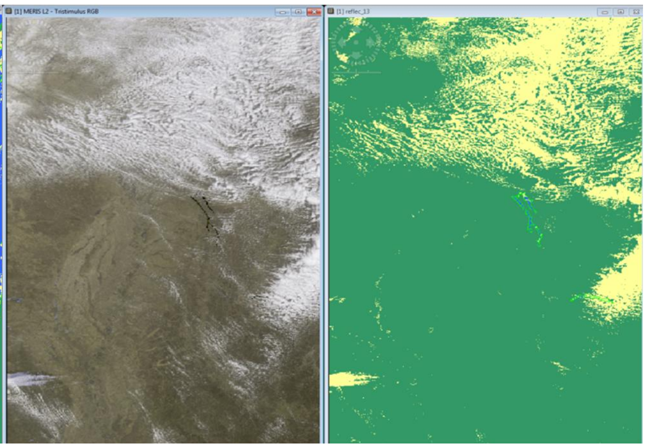

Good cloud detection over land and glint (MER_FRS_2PNUPA20091205_002349)

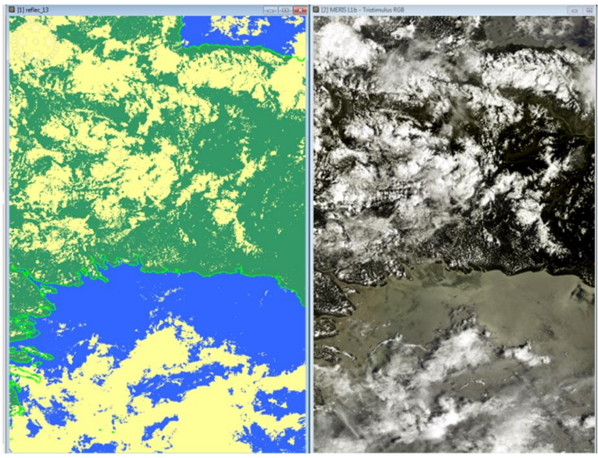

Clouds over snow (MER_FRS_2PNUPA20090509_183603)

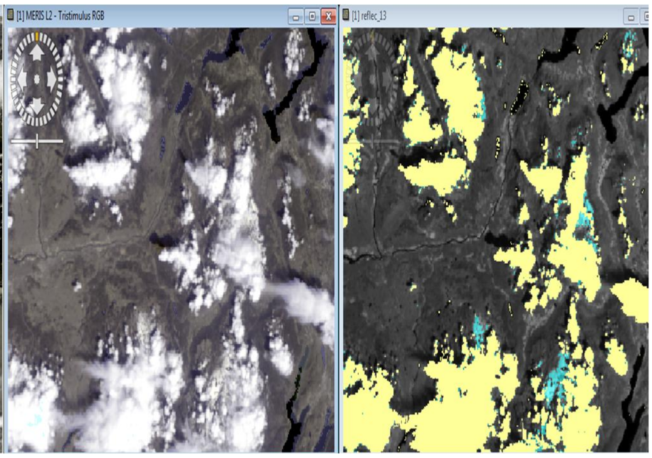

The classification shows a good pixel identification over land and water areas. However, cirrus clouds over land are not well detected in some cases. The lower right example shows the good differentiation between cloud and snow/ice areas over land.

Conclusions

The PixBox investigation as well as the visual inspection of images shows rather good pixel identification for clear water/land/cloud/ice pixels. However, in cases of semi-transparent clouds or mixed pixels containing clouds, it is difficult to judge if it shall be flagged as CLOUD. This depends on the level 2 processing how it deals with such ambiguous cases. Over land, less of these mixed pixels are flagged as CLOUD than over water.

Cirrus clouds detection is the most unreliable test within the cloud screening procedure.

Over land the TOAVI_WS flag is often useful to identify cloud shadows and undetected water bodies.

3.5 Science flags

Parameter	Product type	Impacted by 3rd reprocessing	Contributor
COASTLINE ICE_HAZE SNOW MEDIUM GLINT HIGH GLINT	☐ Ocean product ☐ Cloud product ☐ Land product ☐ Surface classification ☐ Product confidence ☒ Science flag	Yes : ☒ No : ☐	▪ K. Stelzer (BC) ▪ C. Brockmann (BC) ▪ A. Ruescas (BC) ▪ M. Paperin (BC)

Accuracy goal	Estimated quality

Method

The validation of the scientific flags listed above has been performed with the PixBox Dataset. The PixBox dataset is a hand-selected dataset of 110,000 MERIS RR pixels 40,000 MERIS FR pixels which have been classified visually into different surface classes by an expert. The classes cover different cloud classes, clear land/water pixels, snow and ice pixels as well as mixed pixels of different surface types. This dataset has been tested against the flagging of the L2 3rd reprocessing products for assessing the quality of the science flags. The results are presented in a contingency matrix. Further, selected scenes are investigated visually how the flagging is working.

Validation results

Consistency of FLAGS

The correct appearance of flags has been verified using those pixels which are contained in PixBox. As first step the consistency and relationship of the L2 flags is checked. By definition, the surface type flags cloud, land and water are mutually exclusive. The science flags are specific for these three surface types. A new feature introduced in the 3rd reprocessing is the detection of snow and ice. Over land surfaces, this information is stored in a new flags, called SNOW_ICE. Over water this information is used – amongst others – to trigger the ICE_HAZE flag. Over water it is difficult to separate the bright surfaces glint, snow, and clouds. Table 5 provides the information how the concerned MERIS L2 flags are related in form of a confusion matrix, where the numbers in the diagonal indicate how often a single flag is raised in the dataset. The figures aside the diagonal show if two flags can be raised for one pixel. E.g. 9048 pixels of the WATER pixels are flagged as ICE_HAZE, while 5084 of the water pixels are flagged as MED_GLINT. ICE_HAZE and MED_GLINT are raises for 1860 pixels. MED_GLINT and HIGH_GLINT are also raised in parallel for the same pixel in 2373 cases.

Table 5: Confusion matrix of L2_flags

	Surface classification			Science flags			
Flag	CLOUD	LAND	WATER	SNOW_ICE	ICE_HAZE	MED_GLINT	HIGH_GLINT
CLOUD	60604	0	0	0	0	0	0
WATER		32130	0	0	9048	5084	4514
LAND			16454	5877	0	0	0
SNOW_ICE				5877	0	0	0
ICE_HAZE					9048	1860	2373
MED_GLINT						5084	2562
HIGH_GLINT							4514

Analysis of PixBox dataset

COASTLINE

The number of pixels that are flagged as COASTLINE in the PixBox dataset is in total 982. Only regarding cloud free pixels, 86% of the COASTLINE pixels are over land (L2_LAND) and 14% are over water (L2_WATER).

Images show that the COASTLINE which is taken from L1b COASTLINE, is not perfectly matching the land water masking as it is not undergone the spectral re-classification which is applied to land-water classification.

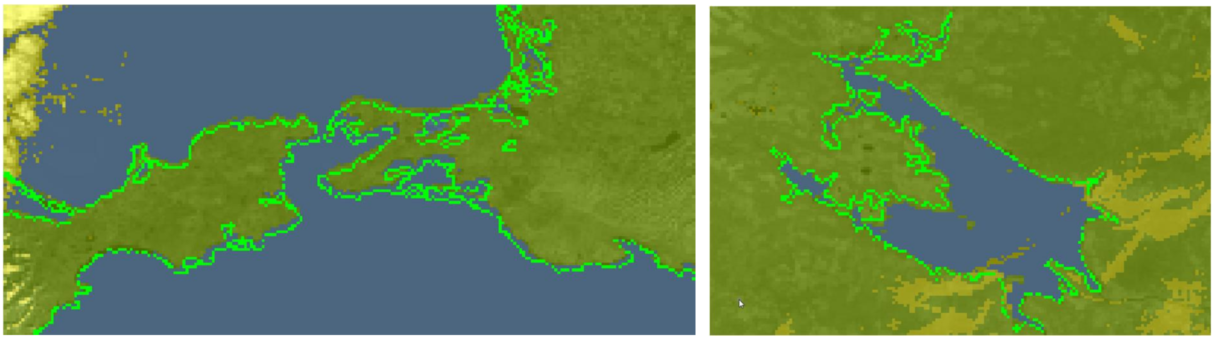

Figure 43: examples of coastline matching with land and water mask.

ICE_HAZE / SNOW_ICE

Figure 44 shows how the snow/ice classified PixBox pixels are flagged by the different L2_flags. Over land, the snow_ice information is stored in the dedicated SNOW_ICE flag, whereas over water, it is triggering the ICE_HAZE flag. In the first pile of Figure 44 we consider all pixels which are truly snow_ice according to the PixPox classification, and study their flagging in the MERIS product: 63% of the pixels are correctly flagged as SNOW_ICE (47%) or ICE_HAZE (13%), while 36% are flagged as CLOUD. If the pixels are flagged as WATER, they are also flagged as ICE_HAZE (except 0.1 %). A very small portion of true SNOW_ICE pixels are classified as clear sky water (0.1%) or clear sky land (0.5%). This can be errors in the PixBox dataset.

When regarding snow/ice pixels under a turbid atmosphere, the portion of the CLOUD flagged pixels becomes larger: 63% are flagged as CLOUD, while 21% are flagged as ICE_HAZE (21%) or SNOW_ICE (16%), respectively for water and land pixels.

For mixed pixels of snow/ice and clouds 61% are flagged as CLOUD and 30% as SNOW_ICE.

Mixed pixels with snow/ice and water are flagged in 87% of the cases as ICE_HAZE while 7% are flagged as CLOUD.

And finally mixed pixels of ice/snow and land are flagged in 38% of the cases as SNOW_ICE, while 35% are flagged as LAND (without SNOW_ICE). 27% are flagged as cloud.

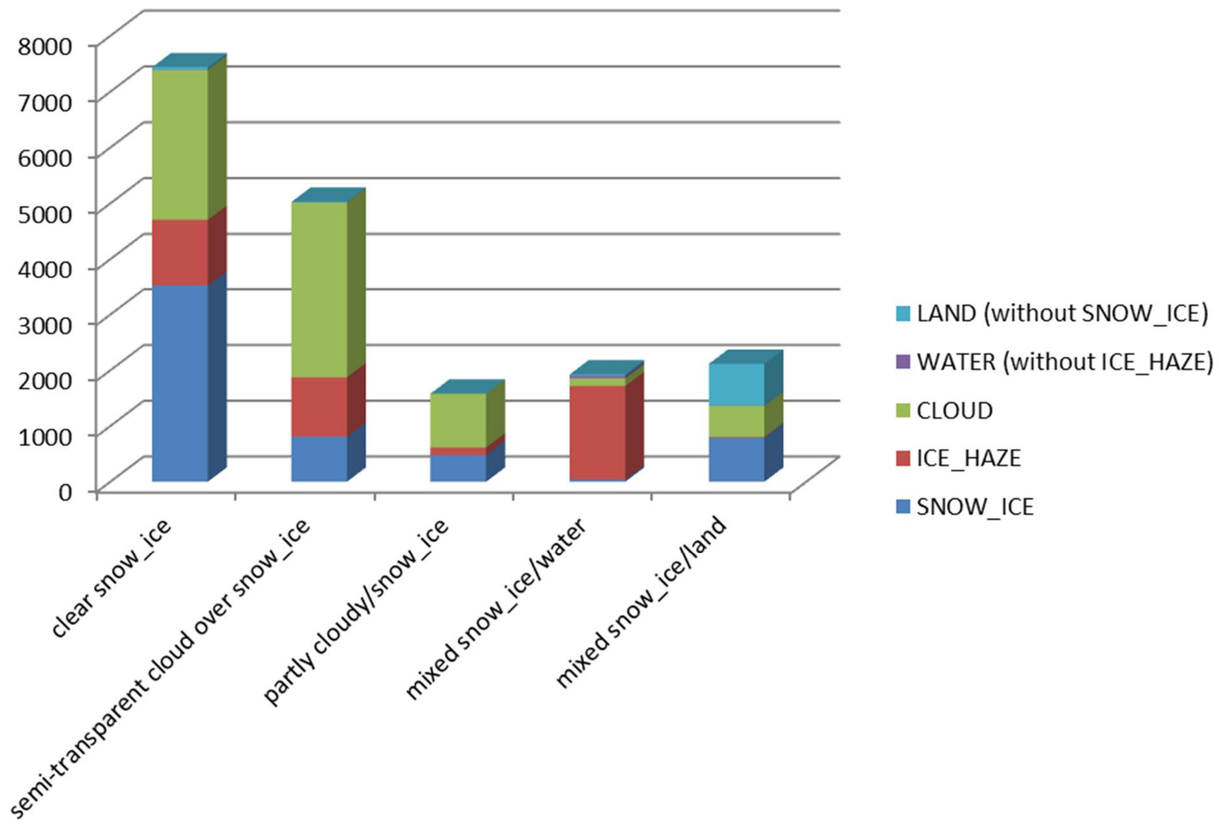

Figure 44: Distribution of L2_flags for clear snow/ice Pixels

GLINT

It has been investigated which L2_flags are raised if the pixels in the PixBox data have been identified as glint. Figure 45 shows that 65% are flagged as MED_GLINT or HIGH_GLINT, while 35% of the pixels are flagged as cloud.

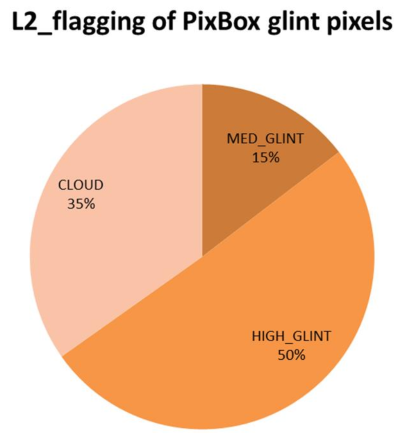

Figure 45: flagging of glint pixels from the PixBox dataset

It has been further investigated, if all pixels that have been flagged as GLINT are also identified as glint in the PixBox dataset. Figure 46 illustrates that 85% of the MED_GLINT flagged pixels and 56% of the HIGH_GLINT flagged pixels are not identified as glint pixels in the PixBox dataset. This has listed in further details in Table 6. This rather large discrepancy is to large extent due to the rather arbitrary – and not comparable - definitions of “glint” in the PixBox dataset, as well as “high” and “medium” glint in L2 flagging.

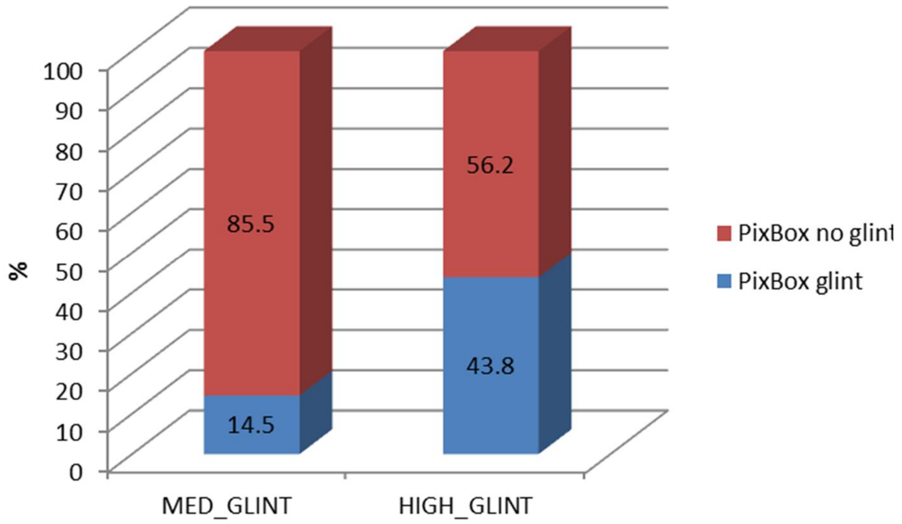

Figure 46: GLINT flagged pixels and PixBox Classification

Table 6: Alignment of MED_GLINT and HIGH_GLINT flagged pixels with PixBox Classification

	glint over clear waters	glint over mixed/turbid atm	no glint clear water	no glint mixed water
MED_GLINT	319	397	1895	2323
HIGH_GLINT	1104	868	1260	1267
CLOUD	760	742	305	9817
WATER, but no GLINT	0	0	5183	16144

<u>Investigation of selected scenes</u>

The following images show some examples of the performance of the flagging on L2 Full Resolution scenes.

Good classification cloud and snow/ice surfaces in L2 FR
(MER_FSG_2PNBCG20091119_101546_000002782084_00237_40371_0001.N1

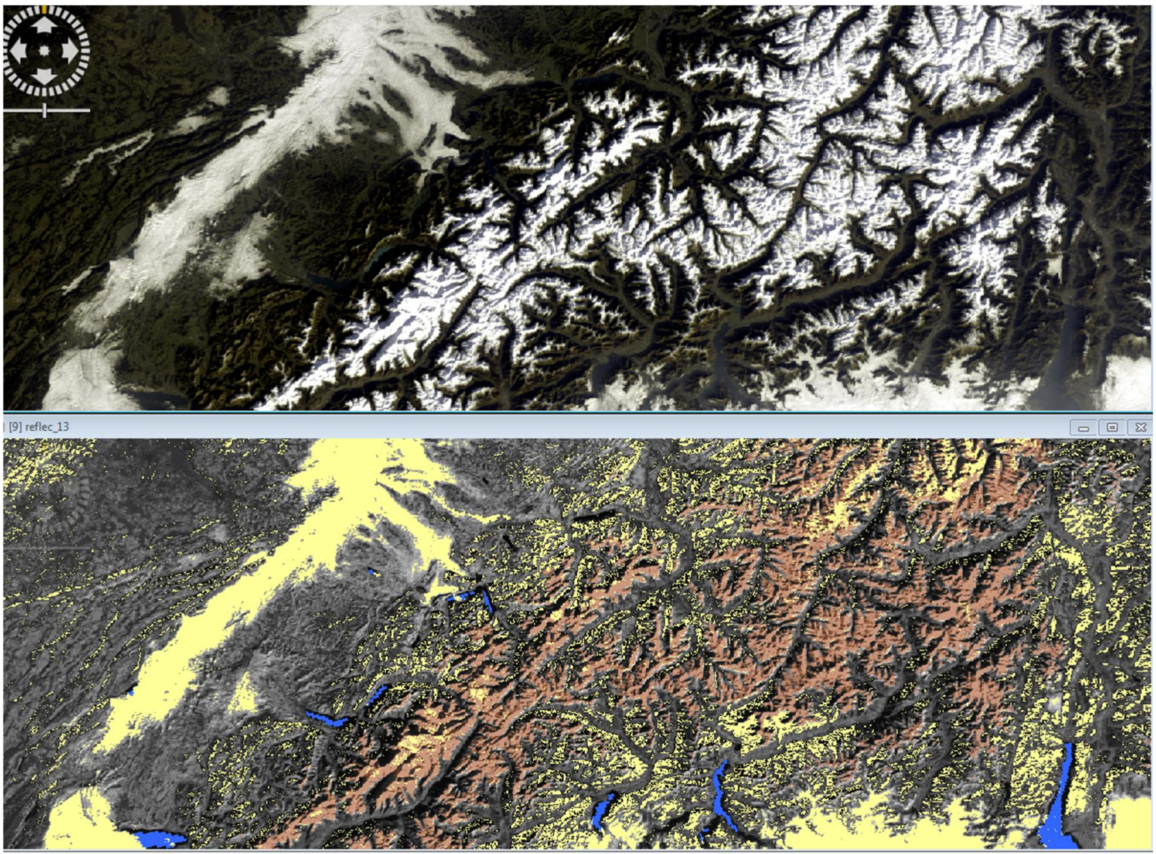

Good cloud and snow/ice discrimination of snow/ice pixels under turbid atmosphere
MER_RR__2PRACR20081216_053632_000026252074_00406_35530_0000.N1

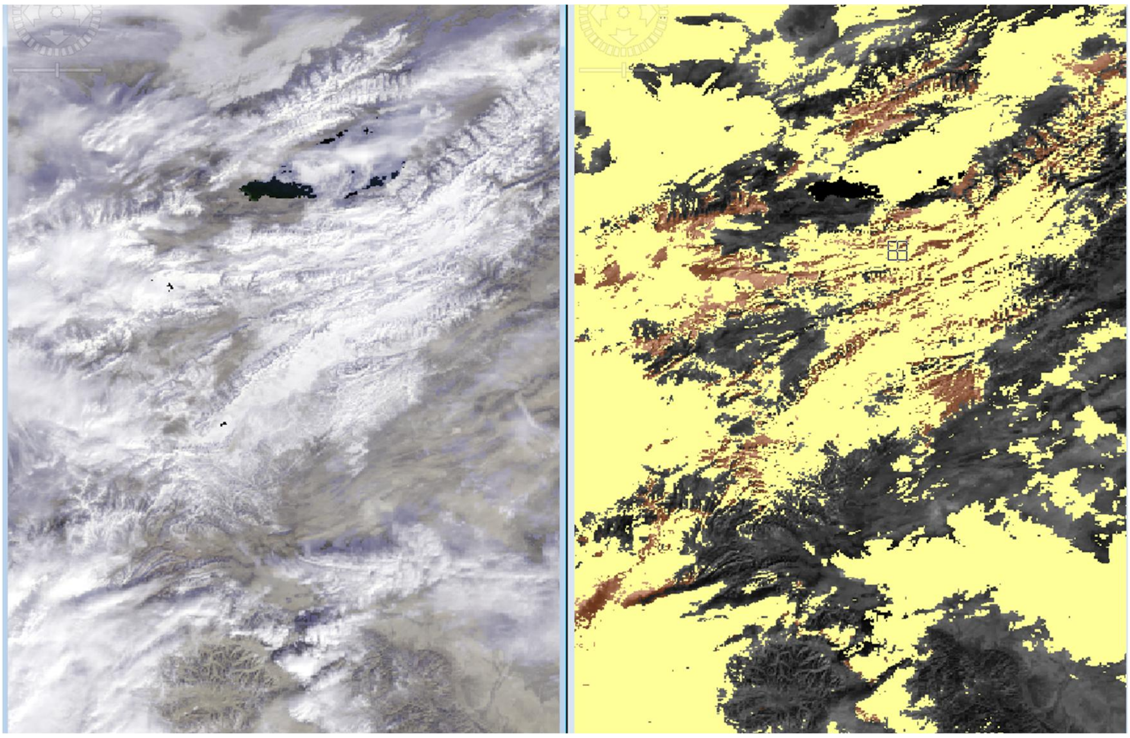

Conclusions

The newly introduced class of flags for ice and snow (SNOW_ICE over land, ICE_HAZE over water) is working as expected. Roughly 2/3 of snow_ice pixels (as identified by an experienced scientist) are flagged as such, while 1/3 is flagged as cloud. Practically no misclassification as land or water occurs. It will be very difficult to further improve the separation between snow and cloud with MERIS due to improper spectral bands for this objective. Pixels with semi-transparent clouds over snow, of spatially mixed snow-cloud pixels are flagged as cloud in 2/3 of the cases, and in 1/3 as SNOW_ICE. Visual inspection of images confirms the overall satisfactory performance of the SNOW_ICE flagging. The evaluation of the GLINT flag is hampered by the obviously different definition of the extend of glint disturbance.

End of document